Electronic Supplementary Information for

Lithium salt of a pro-mesogenic [*closo*-$CB_{11}H_{12}$]$^-$ derivative: Anisotropic Li^+ ion transport in liquid crystalline electrolytes

Litwin Jacob[a], Leszek Niedzicki,[b] Rafał Jakubowski[a], Damian Pociecha,[c] and Piotr Kaszyński*[a,d,e]

[a] Centre of Molecular and Macromolecular Studies, Polish Academy of Sciences, 90-363 Łódź, Poland
[b] Faculty of Chemistry, Warsaw University of Technology, 00-664 Warsaw, Poland
[c] Faculty of Chemistry, University of Warsaw, 02-089 Warsaw, Poland
[d] Faculty of Chemistry, University of Łódź, 91-403 Łódź, Poland
[e] Department of Chemistry, Middle Tennessee State University, Murfreesboro, TN 37130, USA

Table of Content

1. Additional synthetic details..... S2
2. NMR spectra S4
3. DSC measurements S31
4. Additional photomicrographs of LC textures..... S33
5. Powder XRD data..... S35
6. Sample preparation for EIS measurements..... S35
7. EIS measurements..... S38
8. Computational details..... S41
9. References..... S46

1. Additional synthetic details

General procedure for the preparation of ditosylates, 4[n].

To a solution of tetraethylene glycol, $HO(CH_2CH_2O)_4H$ (500 mg, 2.57 mmol), hexaethylene glycol, $HO(CH_2CH_2O)_6H$ (726 mg, 2.57 mmol) or nonaethylene glycol, $HO(CH_2CH_2O)_9H$ (1.07 g, 2.57 mmol) in CH_2Cl_2 (15 mL), triethylamine (2.2 mL, 15.42 mmol) and 4-toluenesulfonyl chloride (98 mg, 5.14 mmol) were added. The reaction mixture was allowed to stir overnight. Water (40 mL) was added into the solution and CH_2Cl_2 layer was extracted (3 × 15 mL). The organic layer was collected and dried (Na_2SO_4) and the solvent was removed in rotary evaporator to get the crude product, which was purified by column chromatography.

Tetraethylene glycol ditosylate (4[4]).[1,2]

The crude product obtained using $HO(CH_2CH_2O)_4H$ (6.1 g, 31.41 mmol), 4-toluenesulfonyl chloride (11.98 g, 68.81 mmol) and triethylamine (26 mL, 188.43 mmol) was purified by column chromatography (SiO_2, CH_2Cl_2/CH_3CN, 4:1) to give 12.5 g (79% yield) of pure **4[4]** as a colourless oil. ^{1}H NMR (400 MHz, $CDCl_3$) δ 7.78 (d, J = 8.4 Hz, 4H), 7.33 (d, J = 8.3 Hz, 4H), 4.14 (d, J = 4.8 Hz, 4H), 3.67 (d, J = 4.8 Hz, 4H), 3.58–3.53 (m, 8H), 2.44 (s, 6H). ^{13}C{^{1}H} NMR (101 MHz, $CDCl_3$) δ 145.0, 133.1, 130.0, 128.1, 70.9, 70.7, 69.4, 68.8, 21.8. HRMS (ESI-TOF) *m/z*: $[M + H]^+$ calcd for $C_{22}H_{31}O_9S_2$: 503.1409, found: 503.1382.

Hexaethylene glycol ditosylate (4[6]).[2]

The crude product obtained using $HO(CH_2CH_2O)_6H$ (4.0 g, 14.17 mmol), 4-toluenesulfonyl chloride (5.40 g, 28.34 mmol) and triethylamine (12 mL, 85.02 mmol) was purified by column chromatography (SiO_2, CH_2Cl_2/EtOAc, 7:3) to give 5.98 g (72% yield) of pure **4[6]** as a colourless oil. ^{1}H NMR (400 MHz, $CDCl_3$) δ 7.79 (d, J = 8.3 Hz, 4H), 7.33 (d, J = 8.0 Hz, 4H), 4.15 (t, J = 4.8 Hz, 4H), 3.67 (t, J = 4.9 Hz, 4H), 3.63–3.56 (m, 16H), 2.44 (s, 6H). ^{13}C{^{1}H} NMR (101 MHz, $CDCl_3$) δ 144.9, 133.1, 130.0, 128.1, 70.9,

70.72, 70.66, 70.62, 69.4, 68.8, 21.8. HRMS (ESI-TOF) *m/z*: $[M + H]^+$ calcd for $C_{26}H_{39}O_{11}S_2$: 591.1934, found: 591.1898.

Nonaethylene glycol ditosylate (4[9]).

The crude product obtained using $HO(CH_2CH_2O)_9H$ (4.0 g, 9.65 mmol), 4-toluenesulfonyl chloride (3.67 g, 19.30 mmol) and triethylamine (8 mL, 57.90 mmol) was purified by column chromatography (SiO_2, CH_2Cl_2/CH_3CN, 3:2) to give 5.05 g (72% yield) of pure **4[9]** as a colourless oil. ^1H NMR (400 MHz, $CDCl_3$) δ 7.78 (d, J = 8.3 Hz, 4H), 7.33 (d, J = 8.1 Hz, 4H), 4.14 (t, J = 5.0, 4H), 3.67 (t, J = 4.8, 4H), 3.64–3.55 (m, 28H), 2.43 (s, 6H). $^{13}C\{^1H\}$ NMR (101 MHz, $CDCl_3$) δ 144.9, 133.1, 129.9, 128.1, 70.8, 70.69, 70.65, 70.60, 69.4, 68.8, 21.8. HRMS (ESI-TOF) *m/z*: $[M + H]^+$ calcd for $C_{32}H_{51}O_{14}S_2$: 723.2720, found: 723.2712.

2. NMR spectra

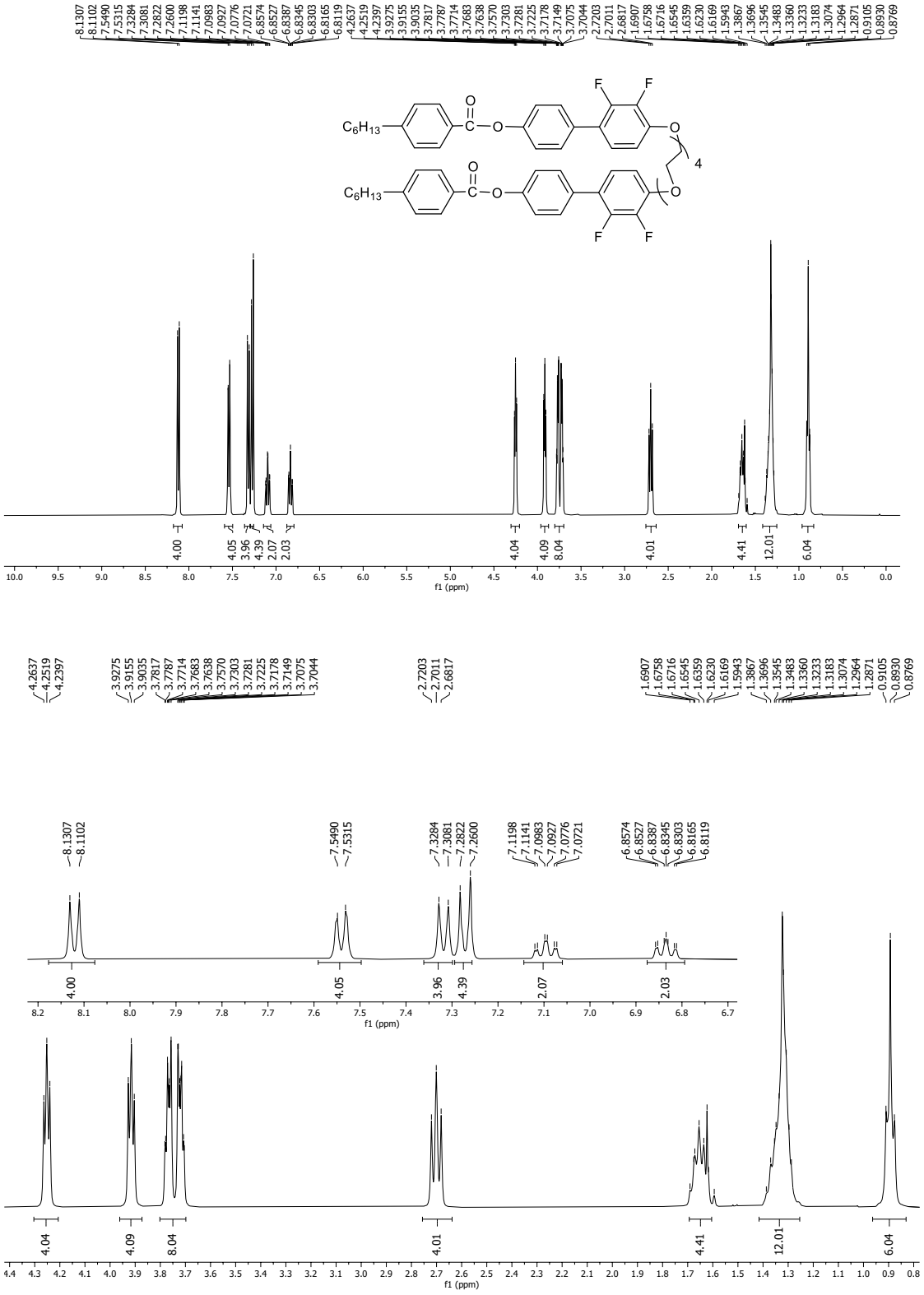

Figure S1. ^{1}H NMR spectrum of **2F[4]** ($CDCl_3$, 400 MHz).

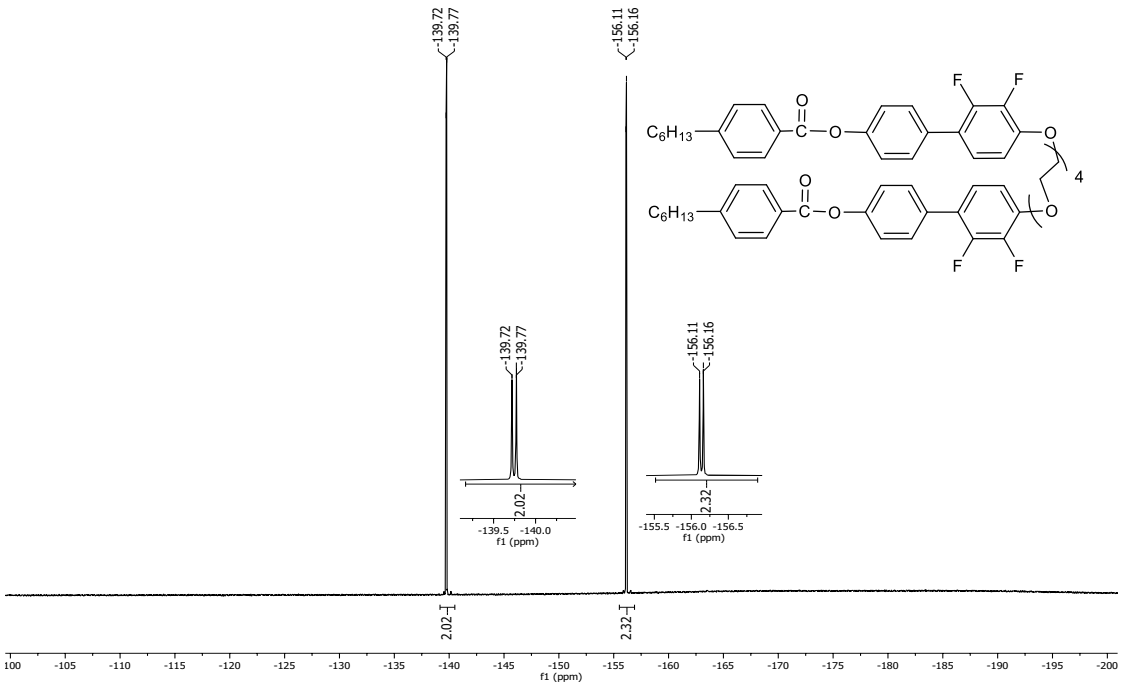

Figure S2. $^{19}F\{^{1}H\}$ NMR spectrum of **2F[4]** ($CDCl_3$, 376 MHz).

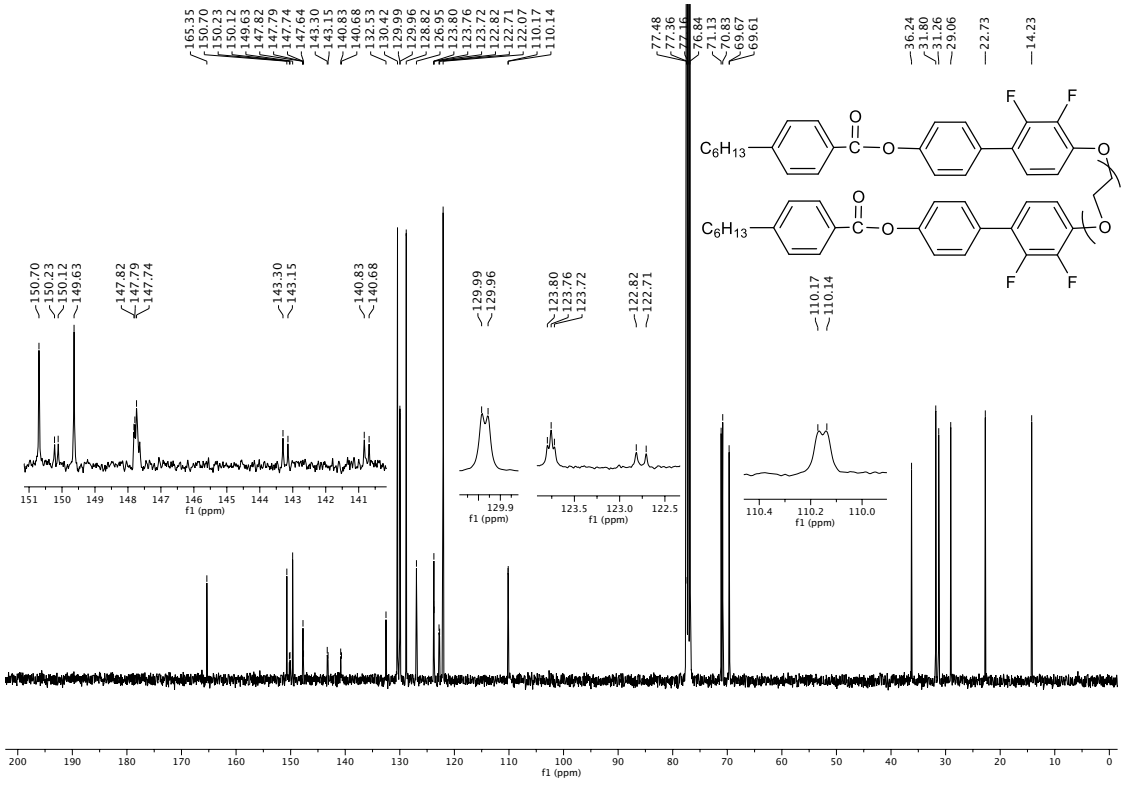

Figure S3. $^{13}C\{^{1}H\}$ NMR spectrum of **2F[4]** ($CDCl_3$, 101 MHz).

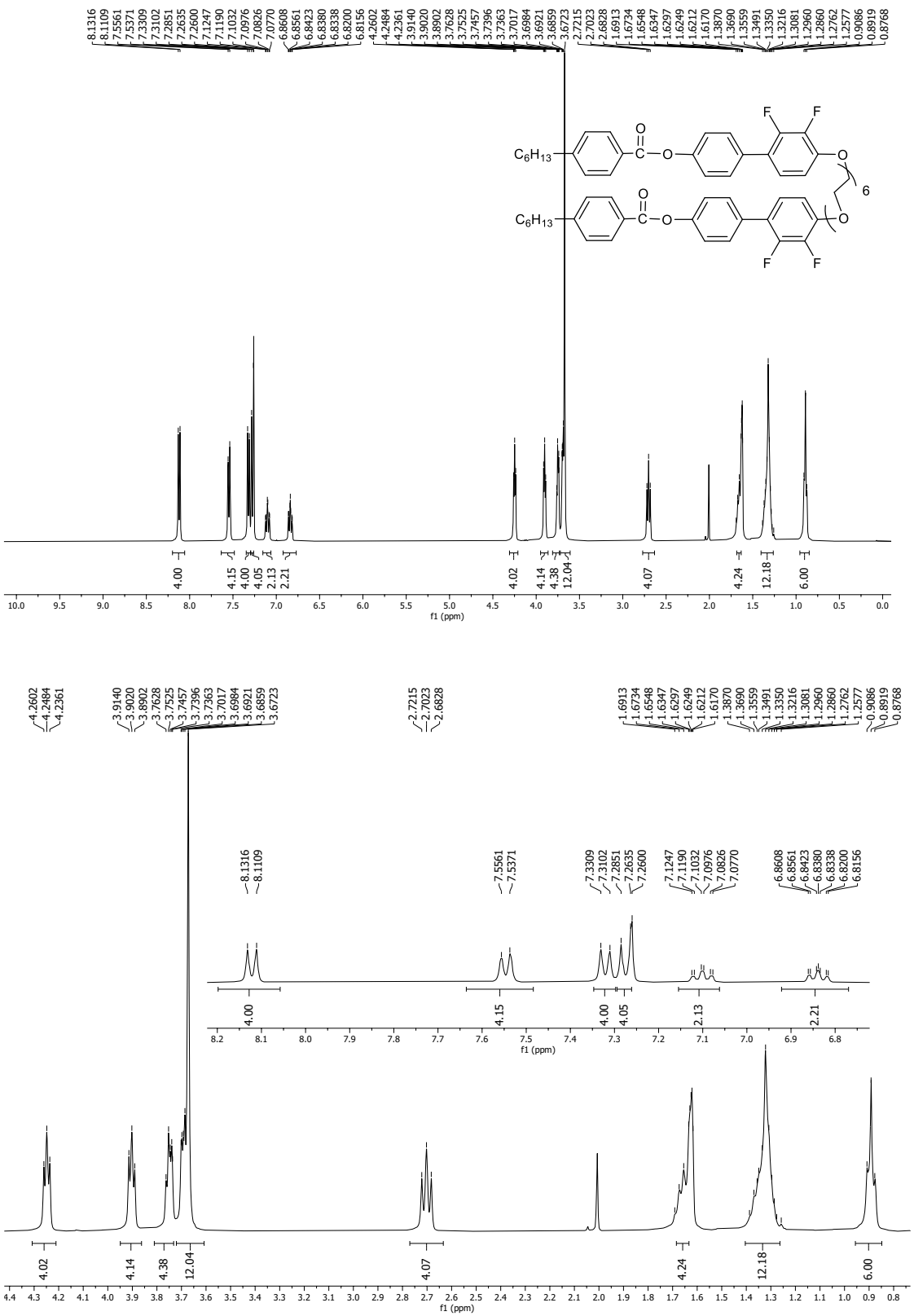

Figure S4. ^{1}H NMR spectrum of **2F[6]** ($CDCl_3$, 400 MHz).

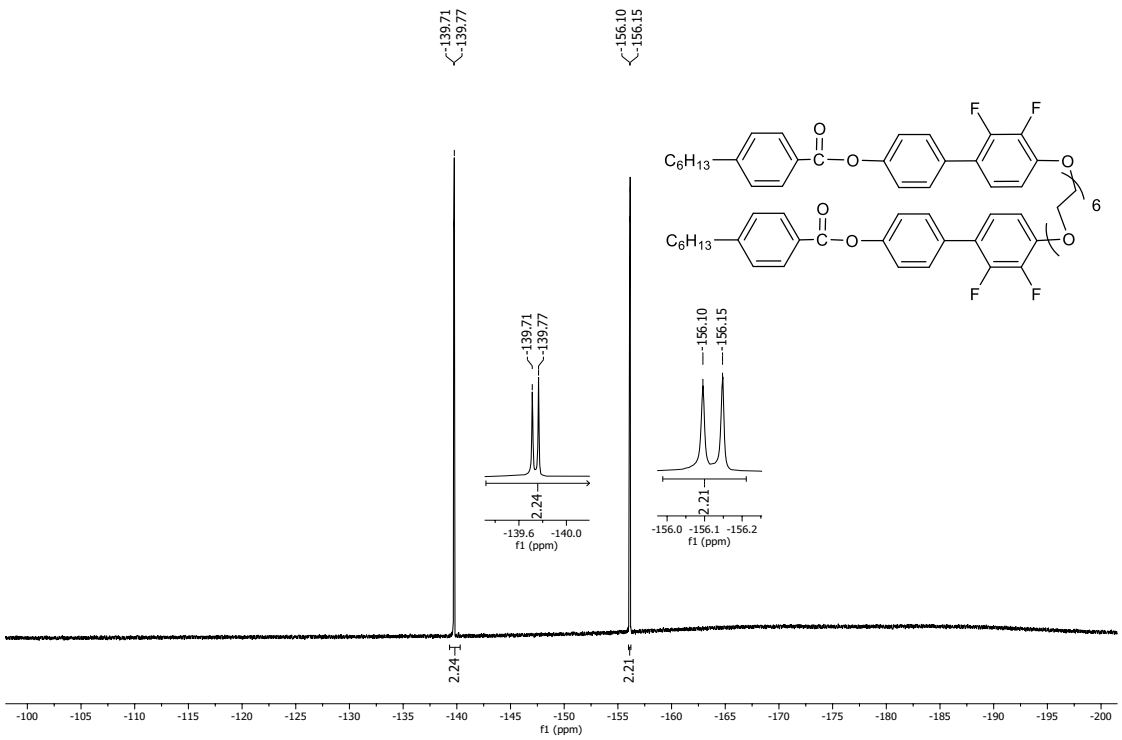

Figure S5. $^{19}F\{^{1}H\}$ NMR spectrum of **2F[6]** ($CDCl_3$, 376 MHz).

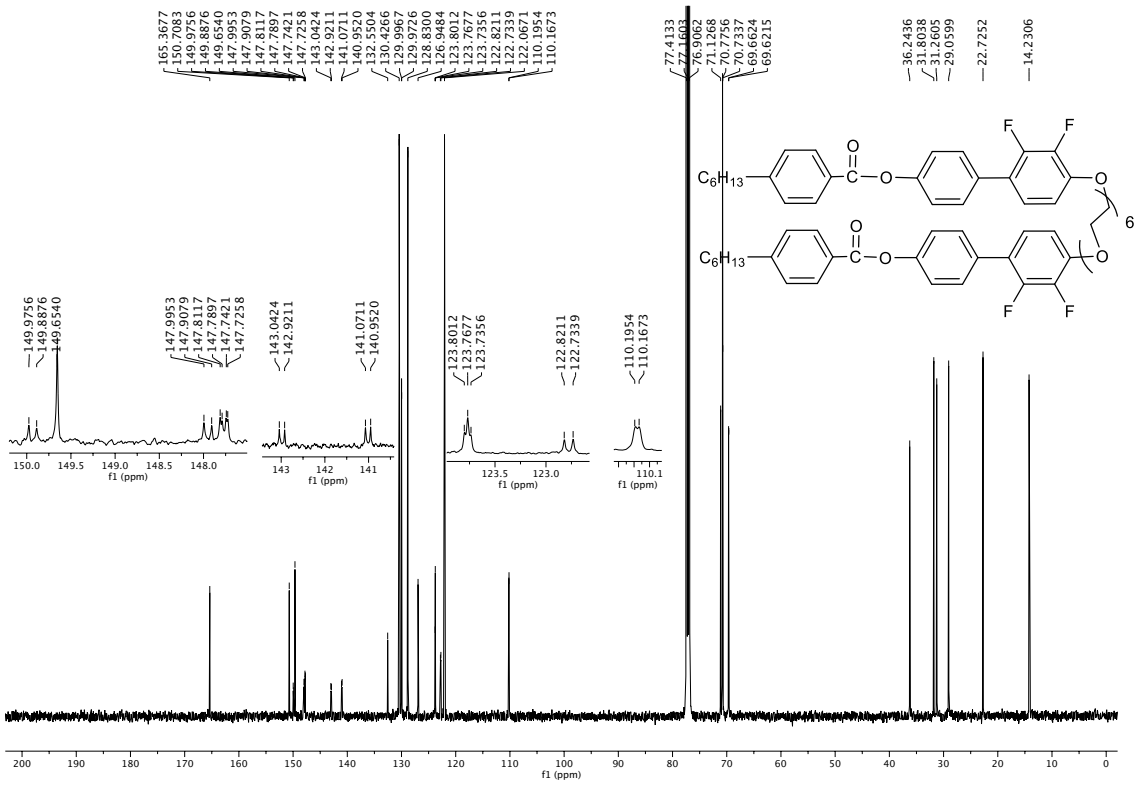

Figure S6. $^{13}C\{^{1}H\}$ NMR spectrum of **2F[6]** ($CDCl_3$, 101 MHz).

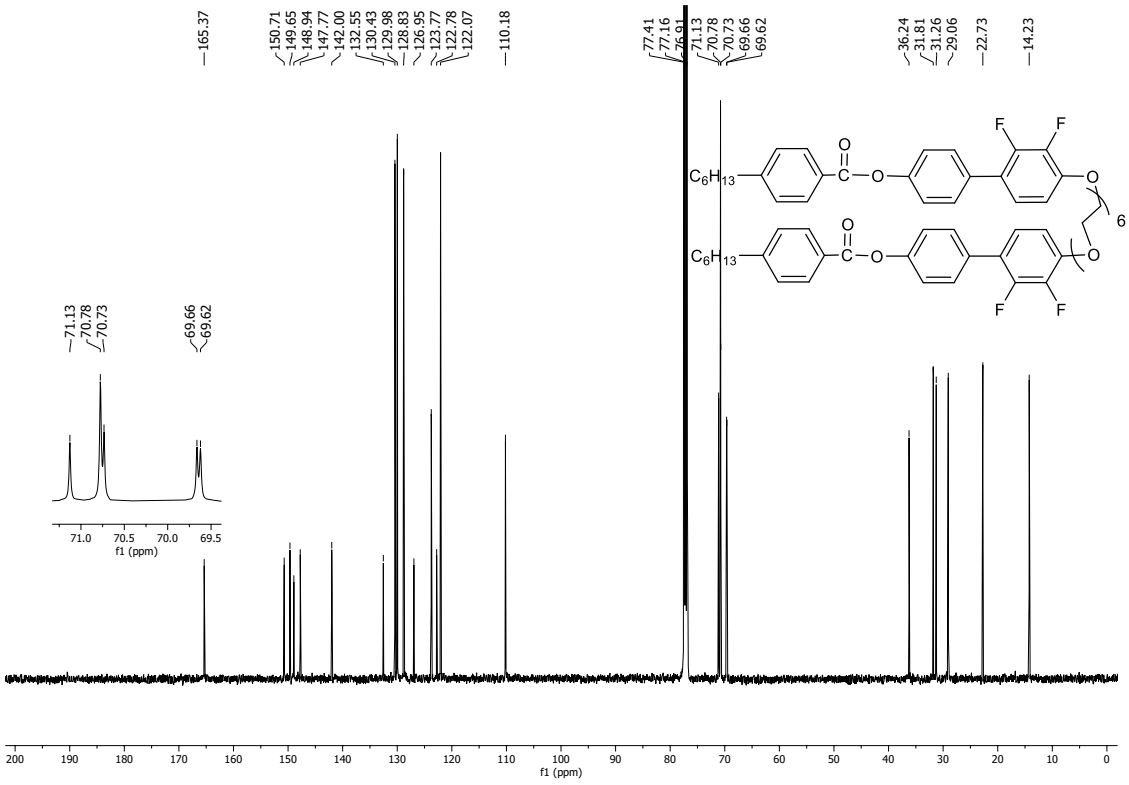

Figure S7. $^{13}C\{^{1}H;^{19}F\}$ NMR spectrum of **2F[6]** ($CDCl_3$, 126 MHz).

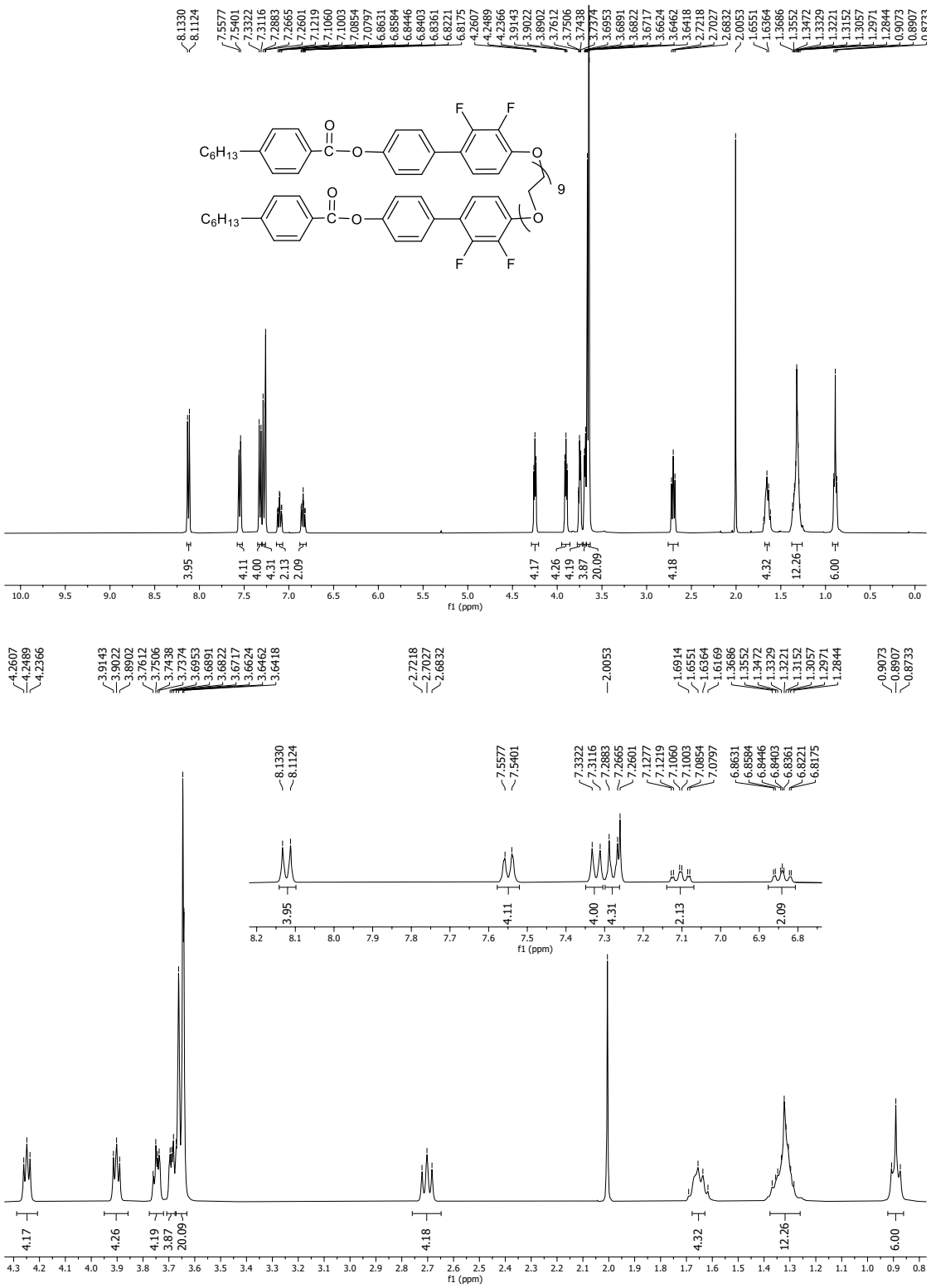

Figure S8. ^{1}H NMR spectrum of **2F[9]** ($CDCl_3$, 400 MHz).

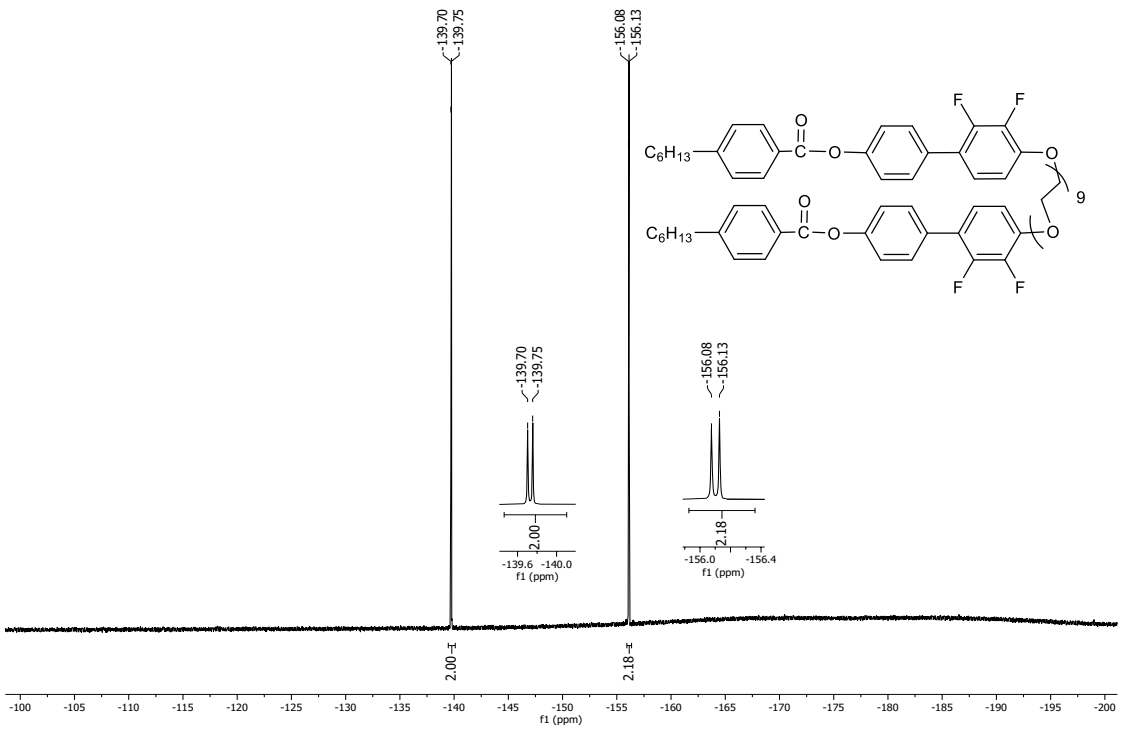

Figure S9. $^{19}F\{^{1}H\}$ NMR spectrum of **2F[9]** ($CDCl_3$, 376 MHz).

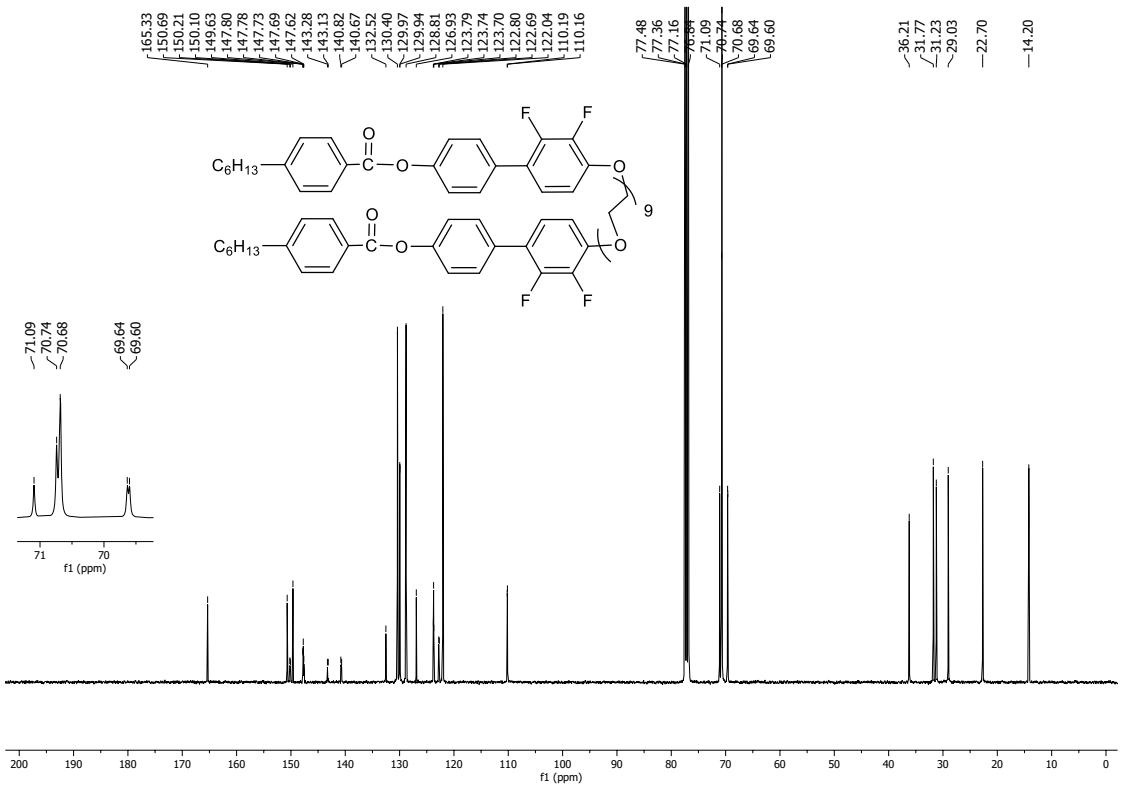

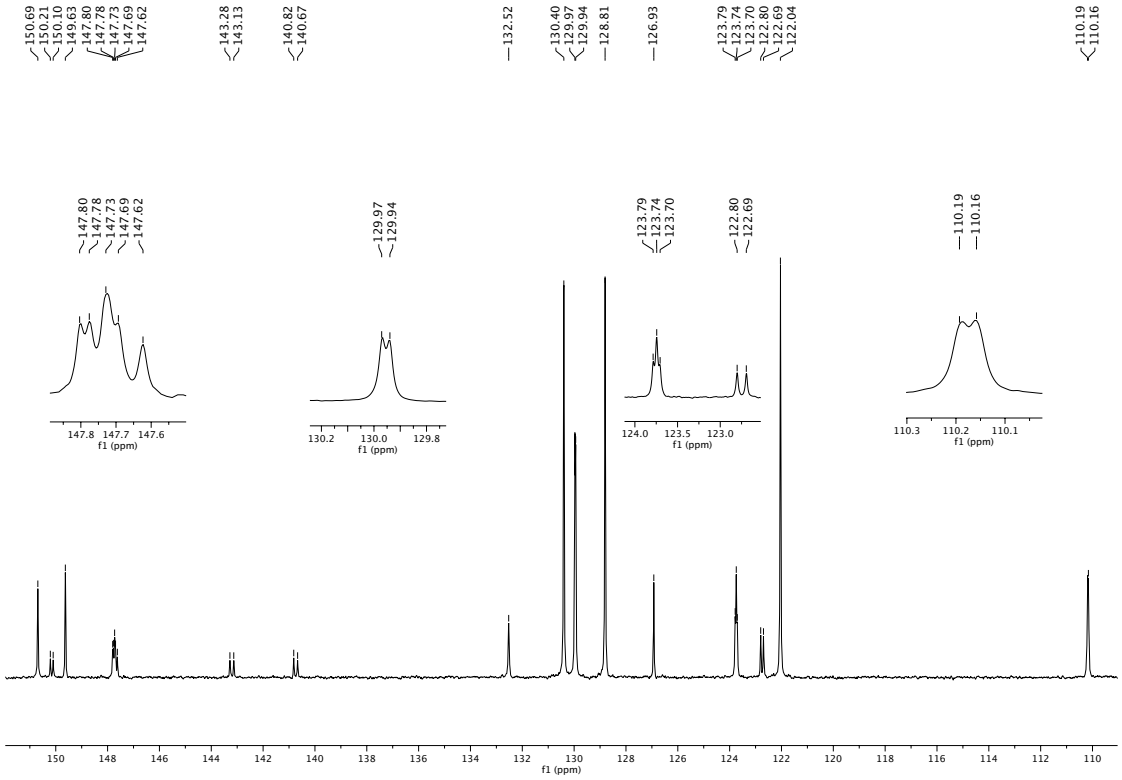

Figure S10. $^{13}C\{^{1}H\}$ NMR spectrum of **2F[9]** ($CDCl_3$, 101 MHz).

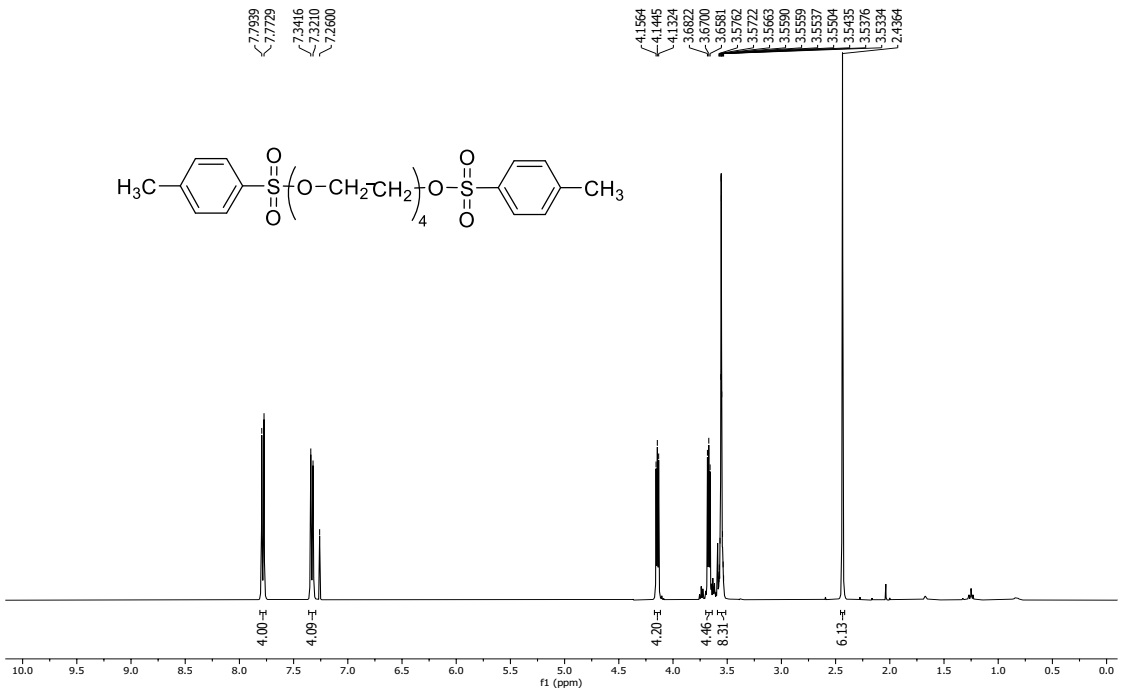

Figure S11. ^{1}H NMR spectrum of **4[4]** ($CDCl_3$, 400 MHz).

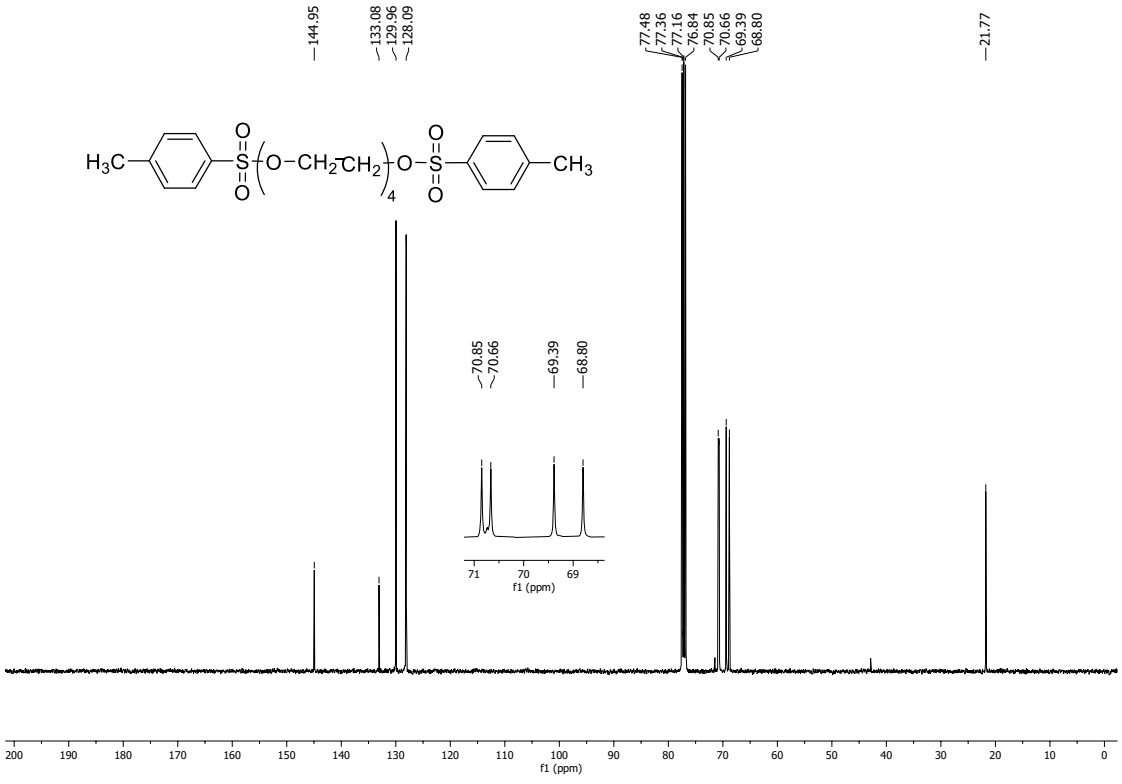

Figure S12. $^{13}C\{^{1}H\}$ NMR spectrum of **4[4]** ($CDCl_3$, 101 MHz).

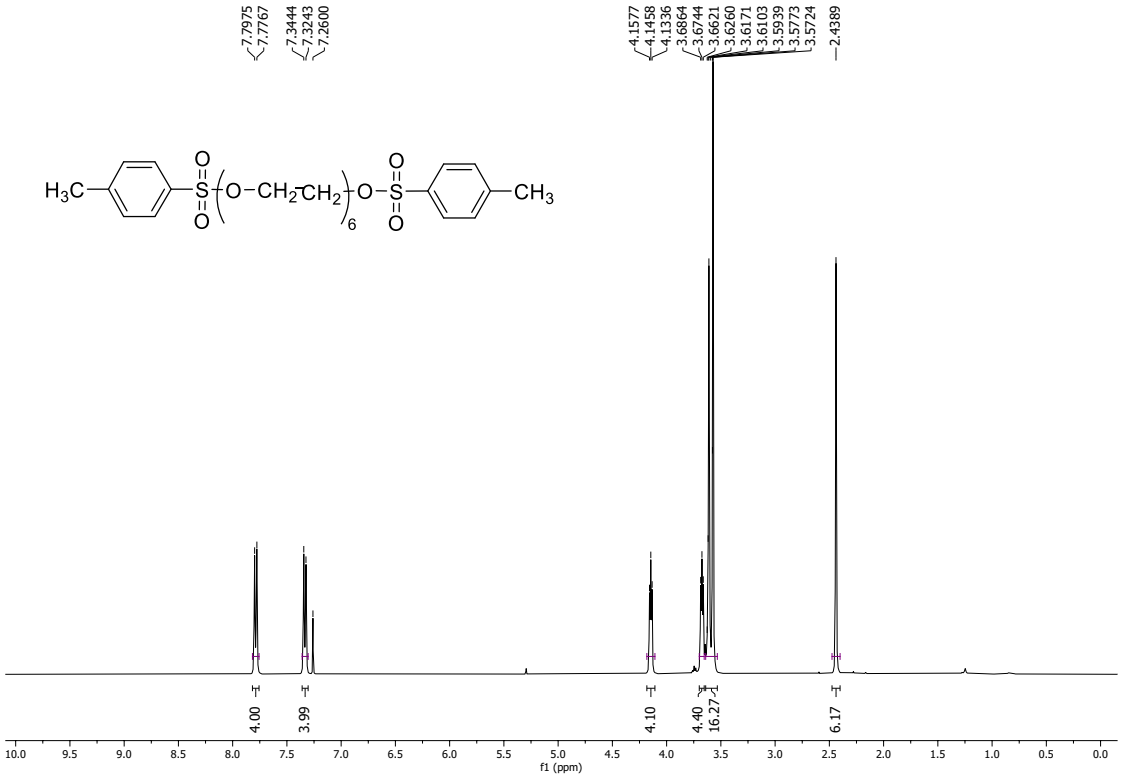

Figure S13. ^{1}H NMR spectrum of **4[6]** ($CDCl_3$, 400 MHz).

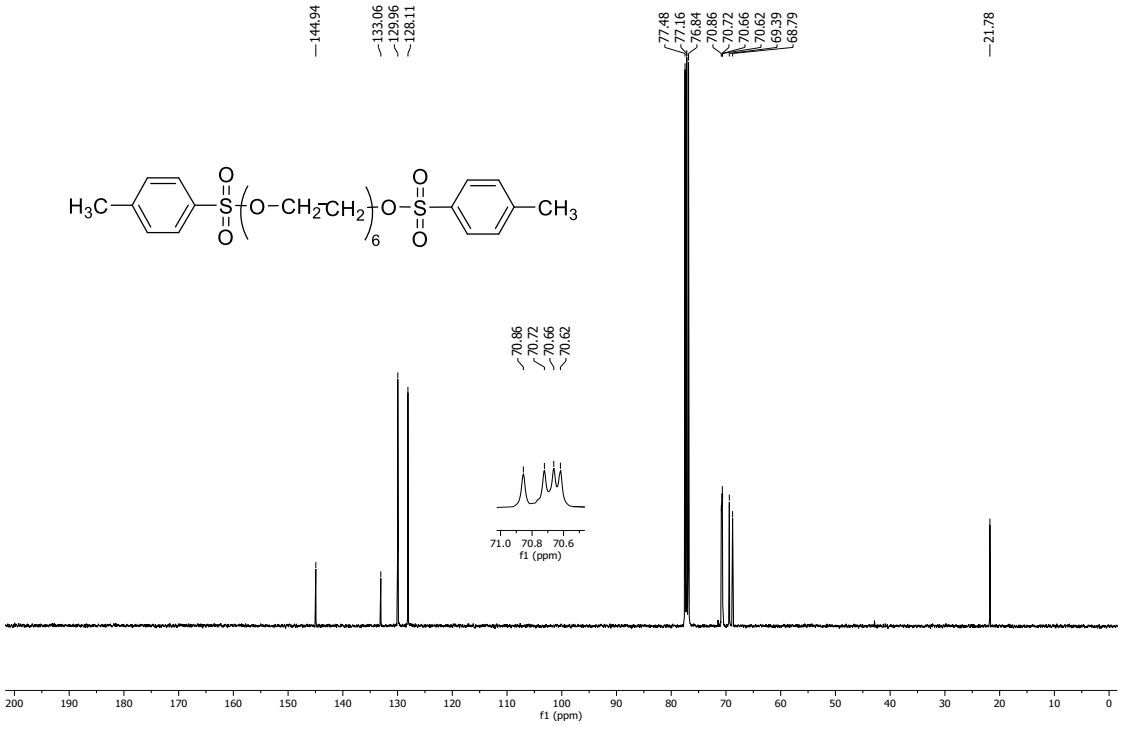

Figure S14. $^{13}C\{^{1}H\}$ NMR spectrum of **4[6]** ($CDCl_3$, 101 MHz).

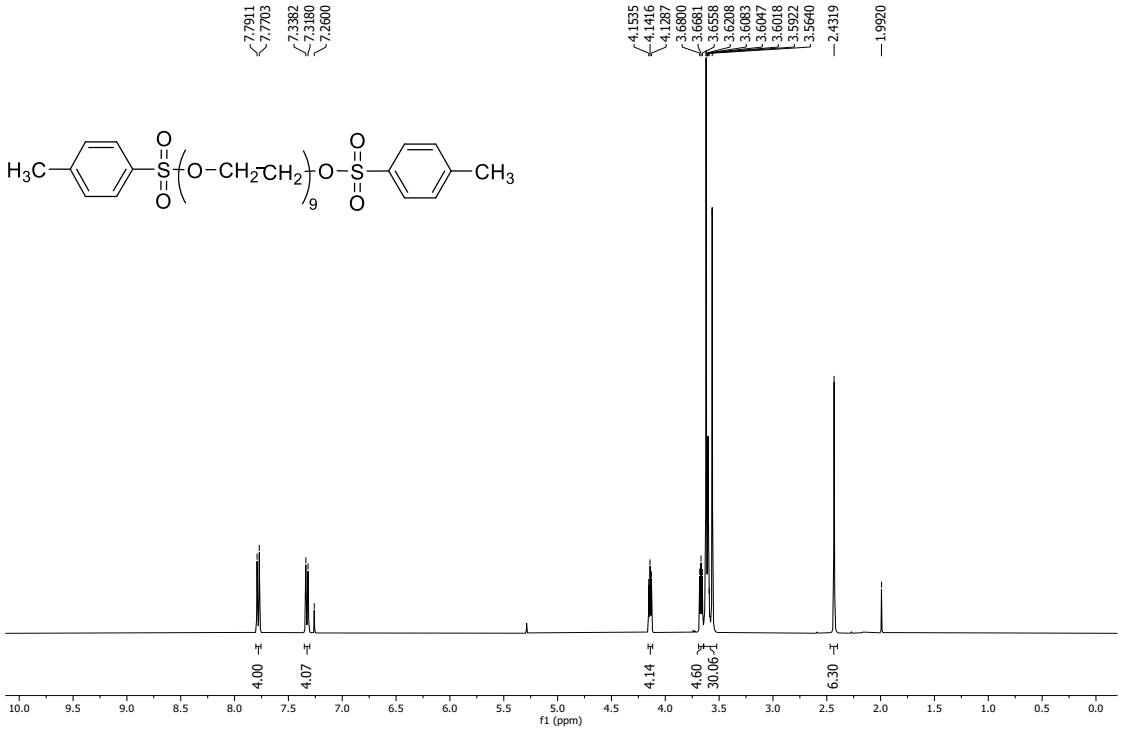

Figure S15. ^{1}H NMR spectrum of **4[9]** ($CDCl_3$, 400 MHz).

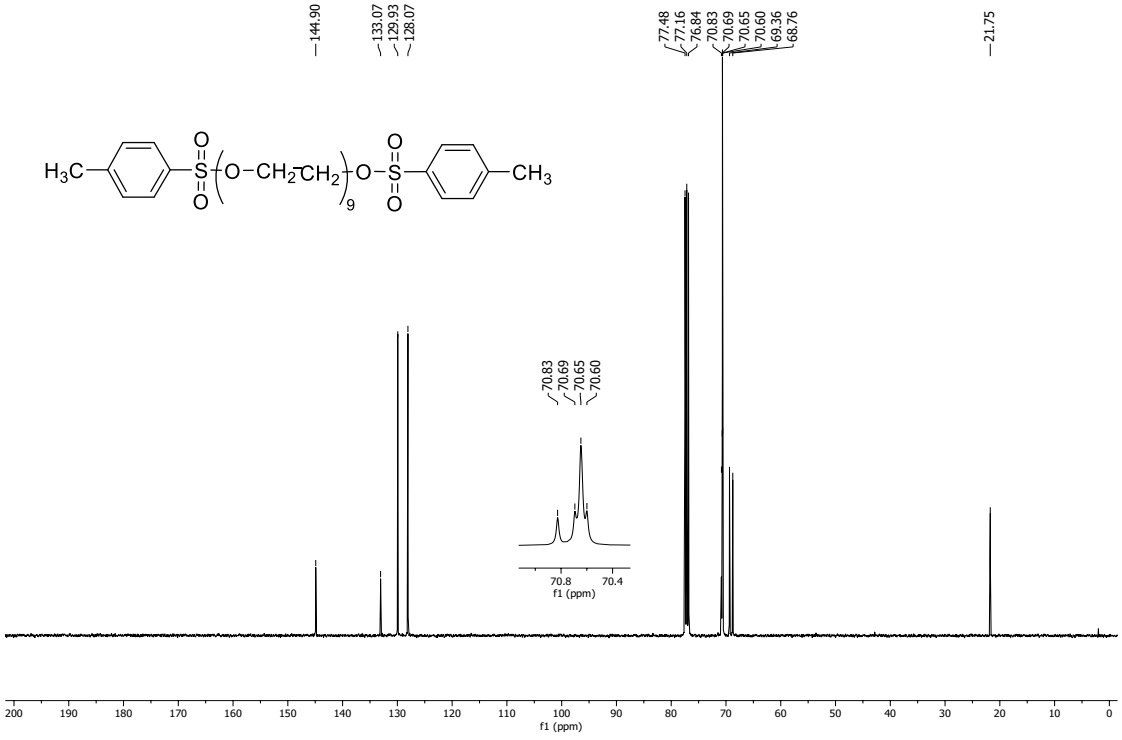

Figure S16. $^{13}C\{^{1}H\}$ NMR spectrum of **4[9]** ($CDCl_3$, 101 MHz).

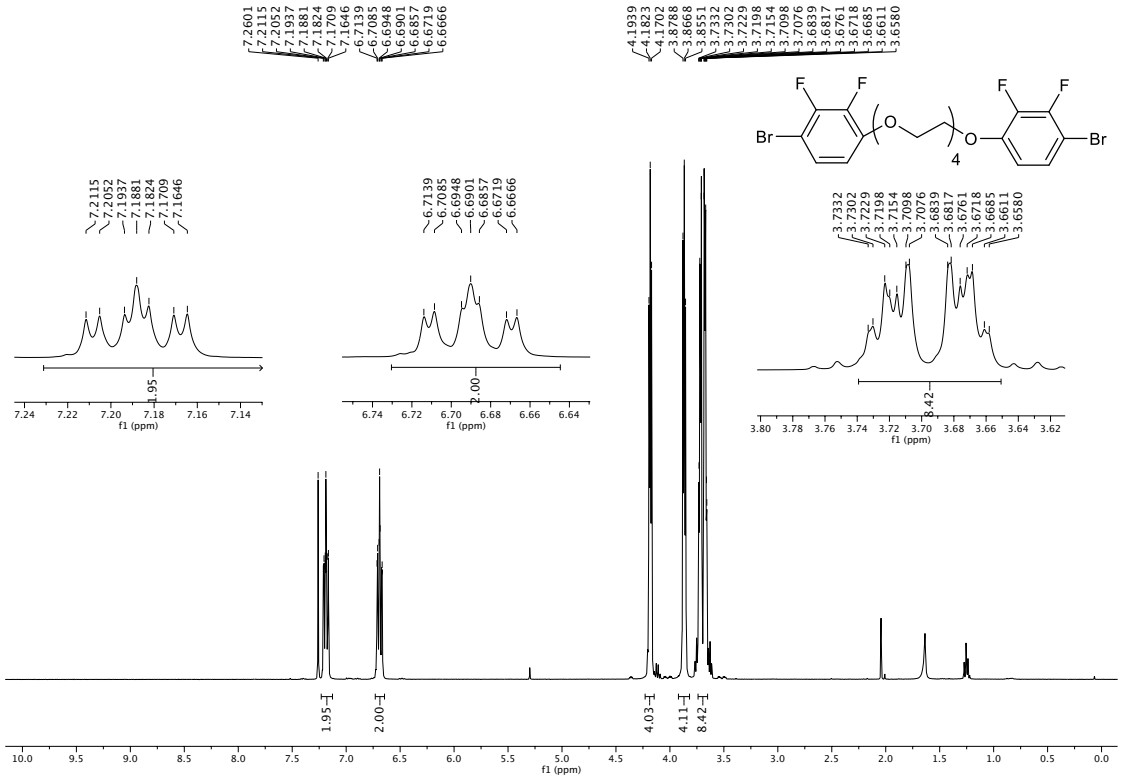

Figure S17. ^{1}H NMR spectrum of **5[4]** ($CDCl_3$, 400 MHz).

Figure S18. $^{19}F\{^{1}H\}$ NMR spectrum of **5[4]** ($CDCl_3$, 376 MHz).

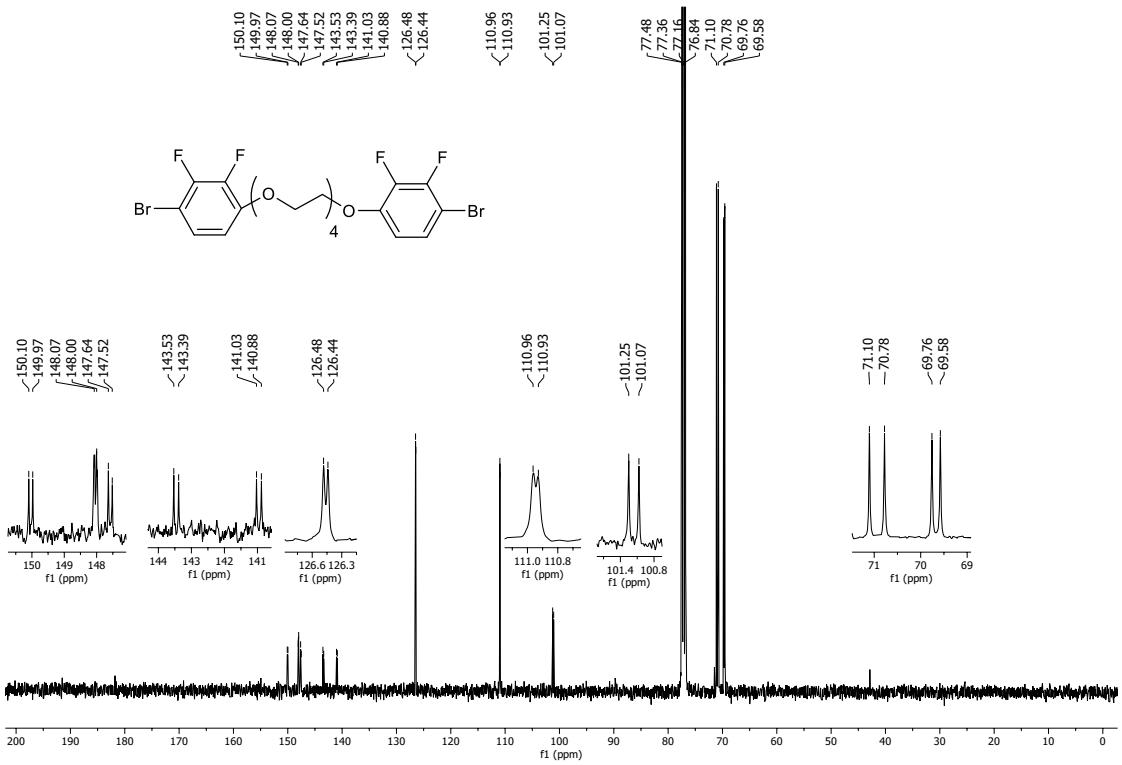

Figure S19. $^{13}C\{^{1}H\}$ NMR spectrum of **5[4]** ($CDCl_3$, 101 MHz).

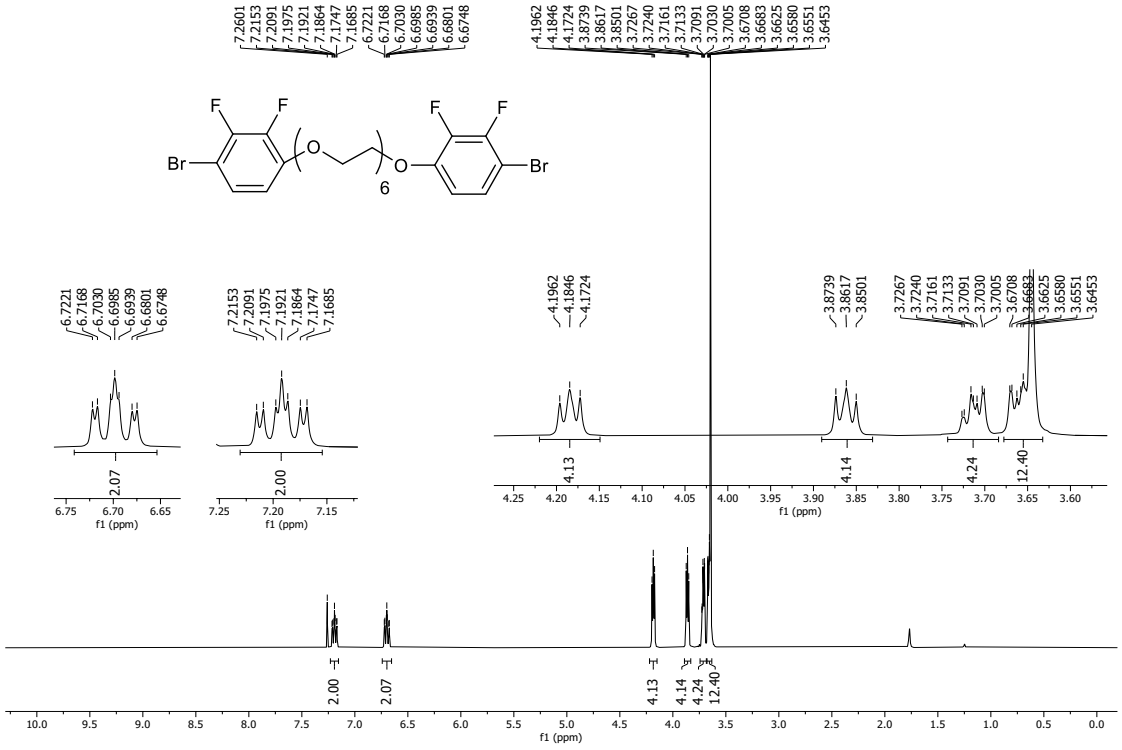

Figure S20. ^{1}H NMR spectrum of **5[6]** ($CDCl_3$, 400 MHz).

Figure S21. $^{19}F\{^{1}H\}$ NMR spectrum of **5[6]** ($CDCl_3$, 376 MHz).

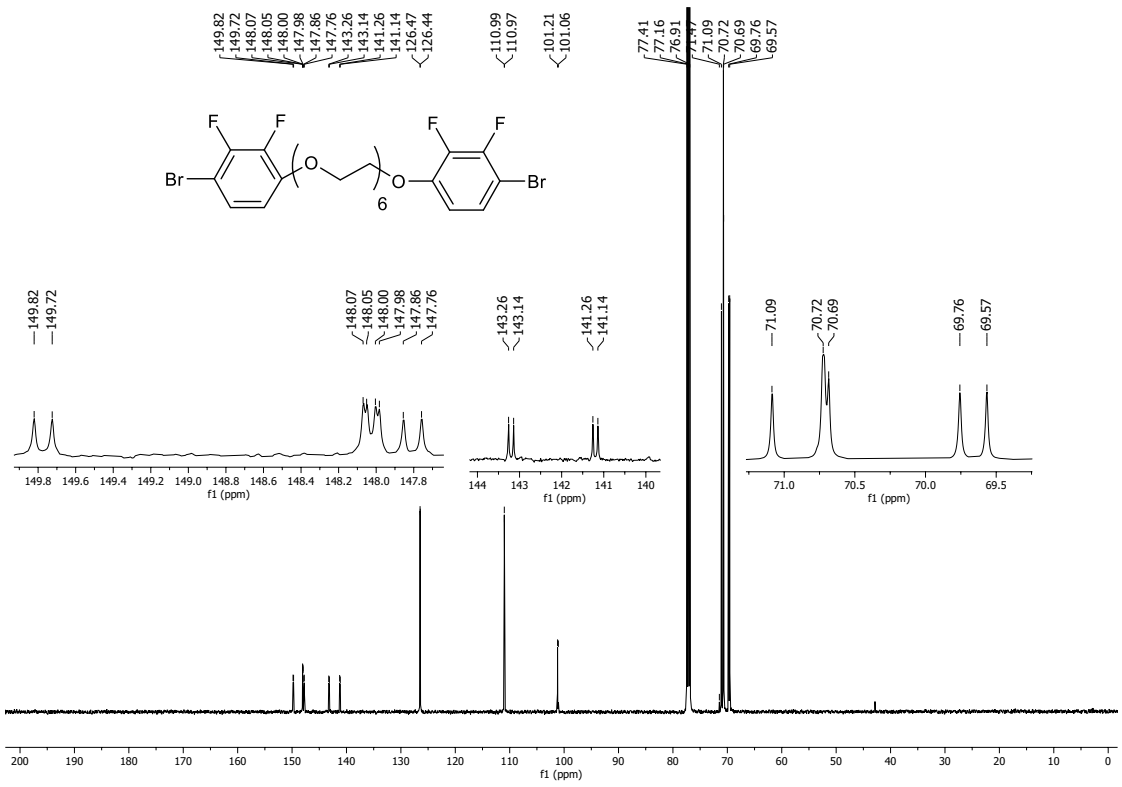

Figure S22. $^{13}C\{^{1}H\}$ NMR spectrum of **5[6]** ($CDCl_3$, 126 MHz).

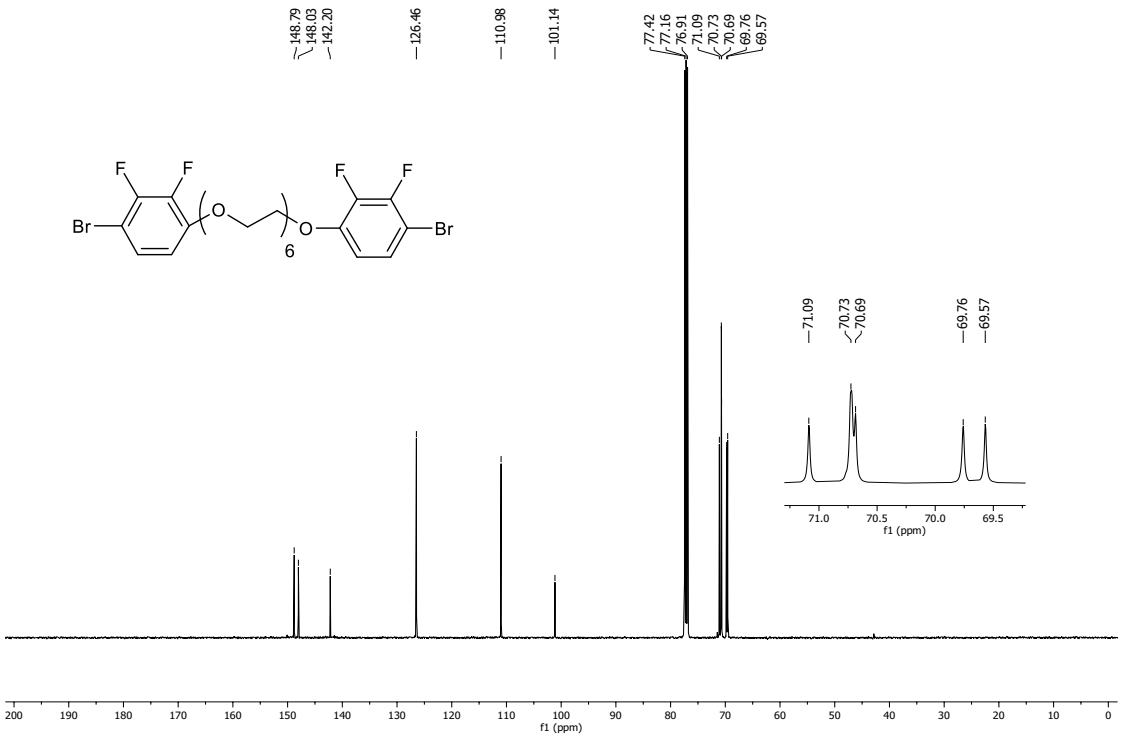

Figure S23. $^{13}C\{^{1}H;^{19}F\}$ NMR spectrum of **5[6]** ($CDCl_3$, 126 MHz).

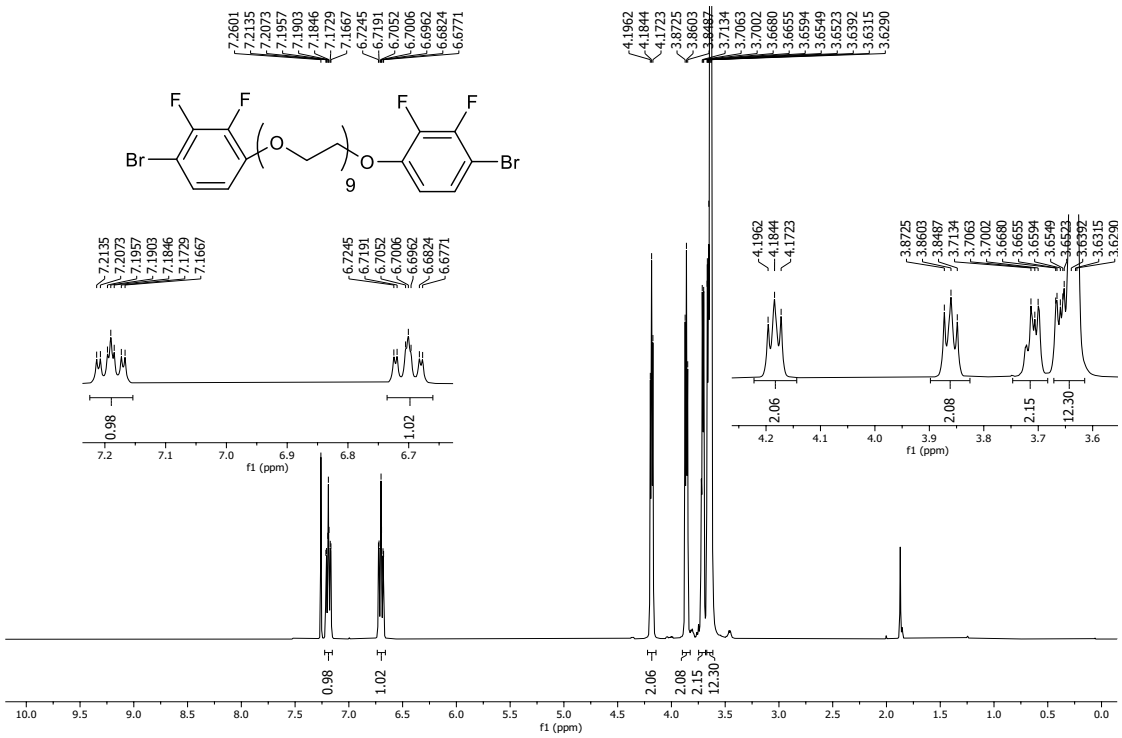

Figure S24. ^{1}H NMR spectrum of **5[9]** ($CDCl_3$, 400 MHz).

Figure S25. $^{19}F\{^{1}H\}$ NMR spectrum of **5[9]** ($CDCl_3$, 376 MHz).

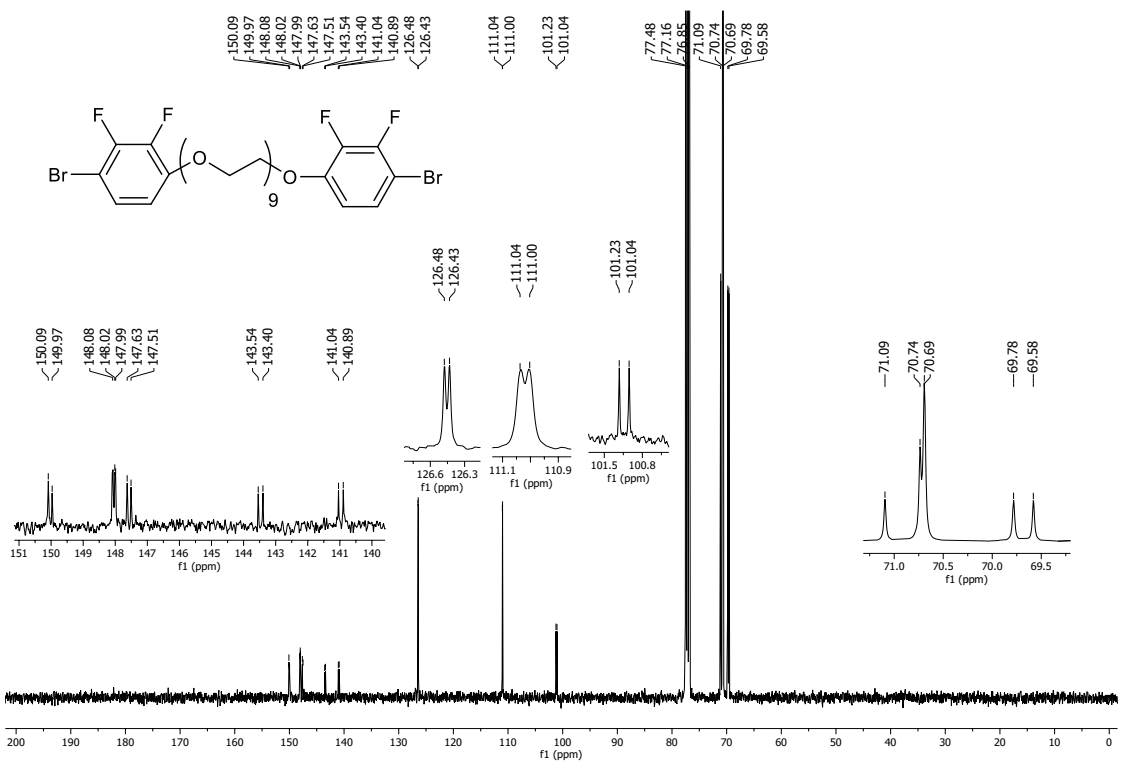

Figure S26. $^{13}C\{^{1}H\}$ NMR spectrum of **5[9]** ($CDCl_3$, 101 MHz).

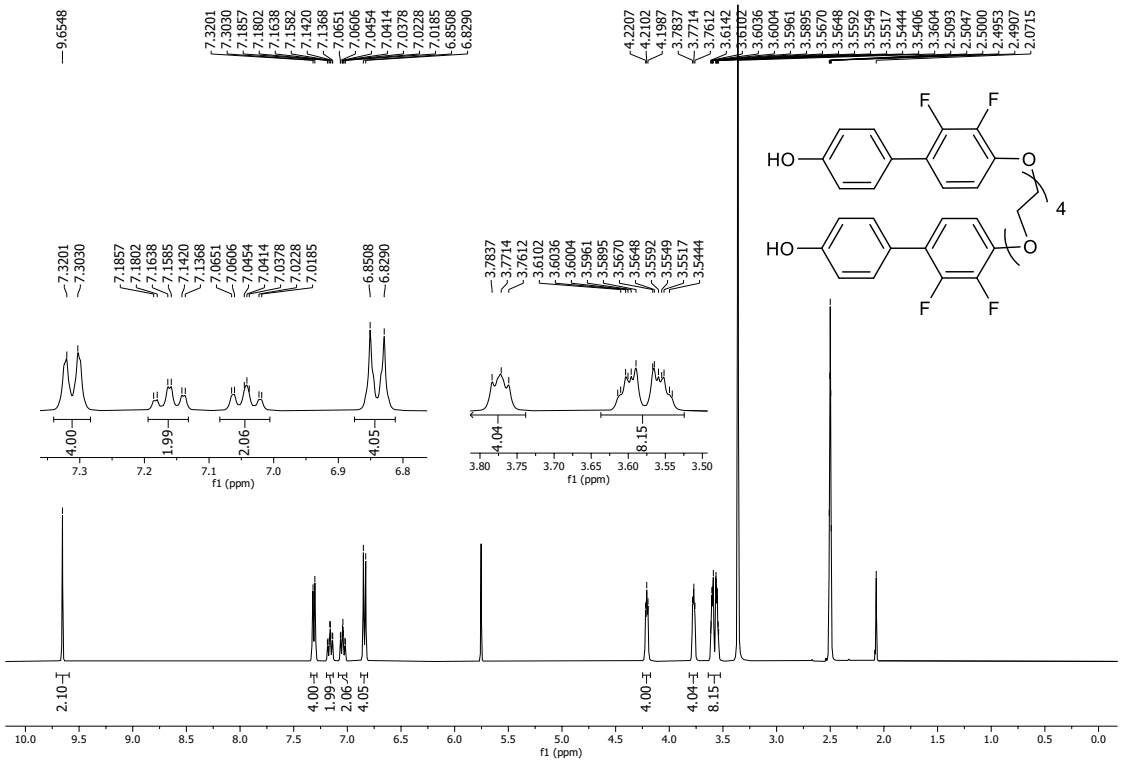

Figure S27. ^{1}H NMR spectrum of **6[4]** (DMSO-d_6, 400 MHz).

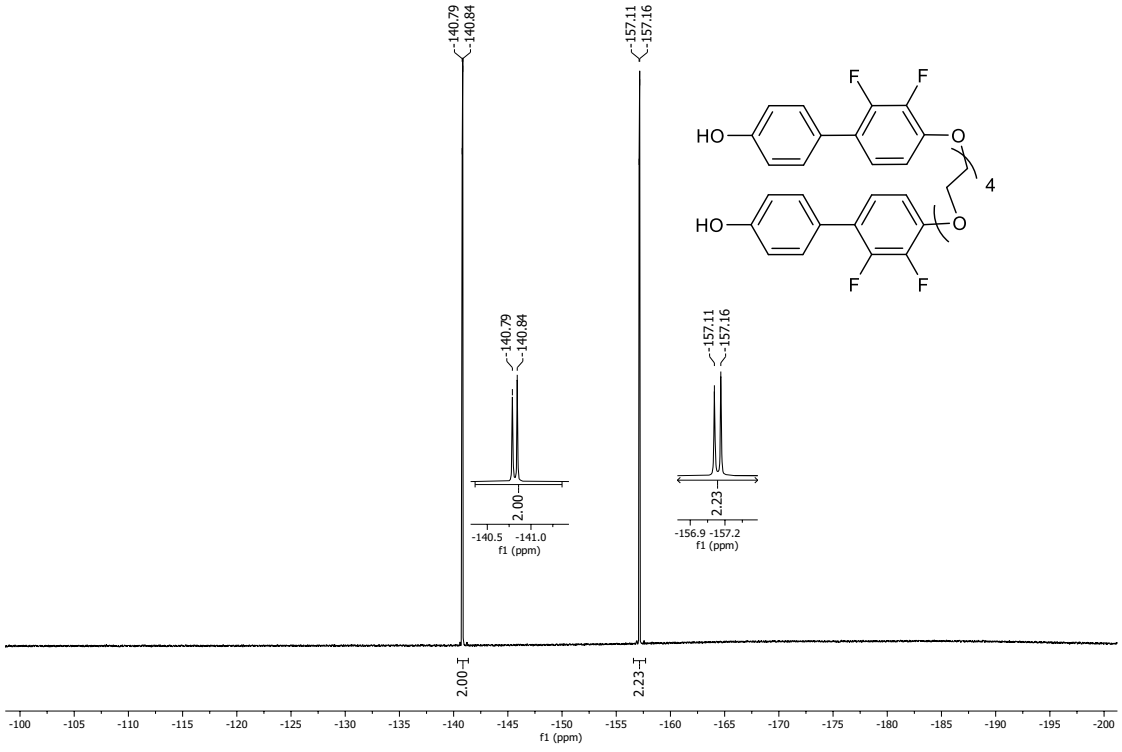

Figure S28. ^{19}F{^{1}H} NMR spectrum of **6[4]** (DMSO-d_6, 376 MHz).

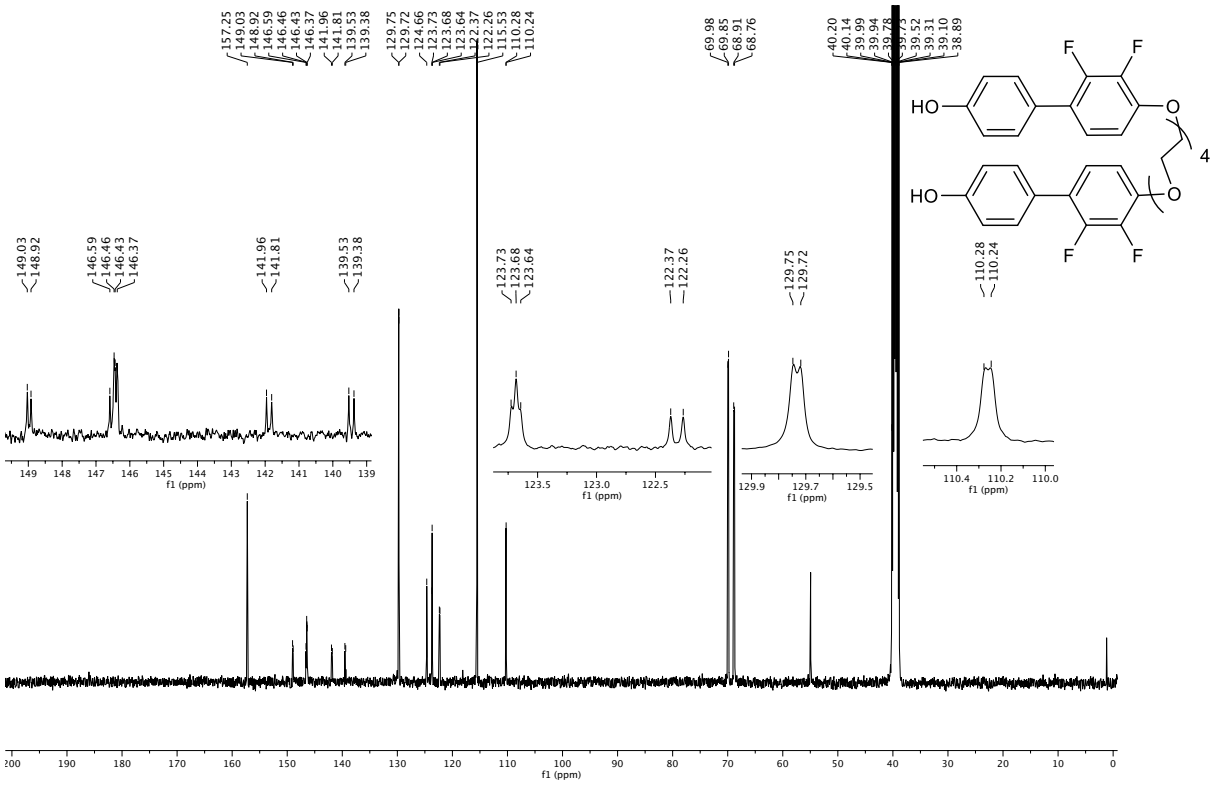

Figure S29. $^{13}C\{^{1}H\}$ NMR spectrum of **6[4]** (DMSO-d_6, 101 MHz).

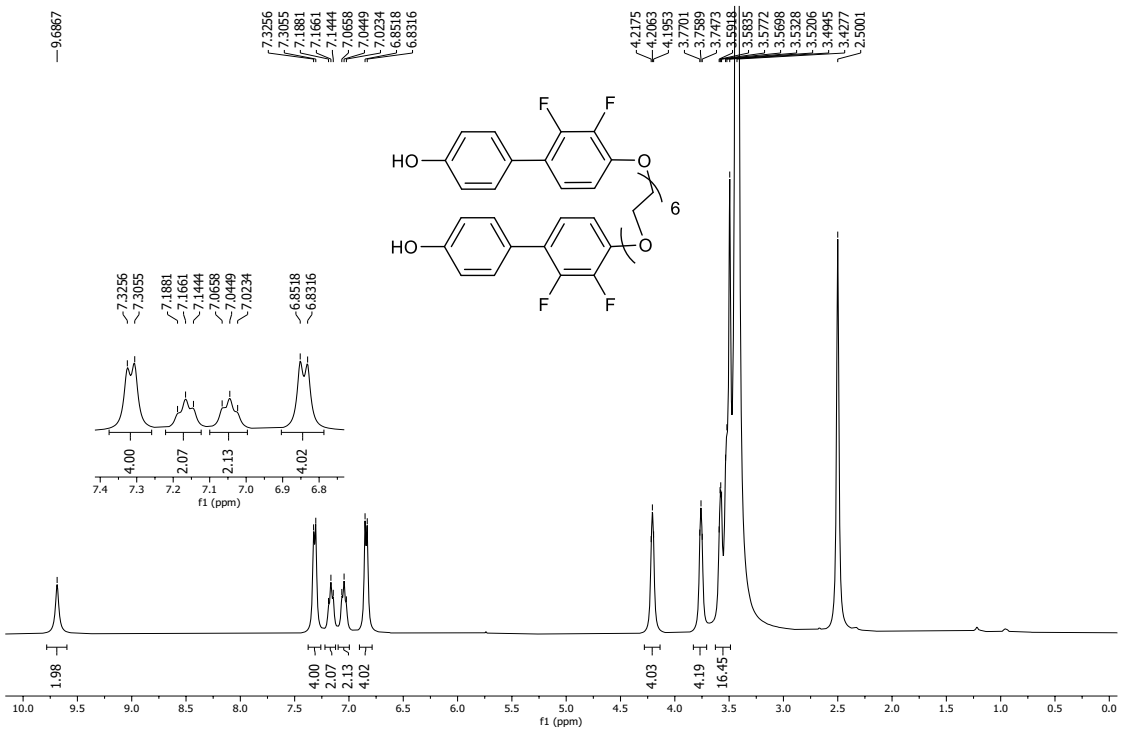

Figure S30. ^{1}H NMR spectrum of **6[6]** (DMSO-d_6, 400 MHz).

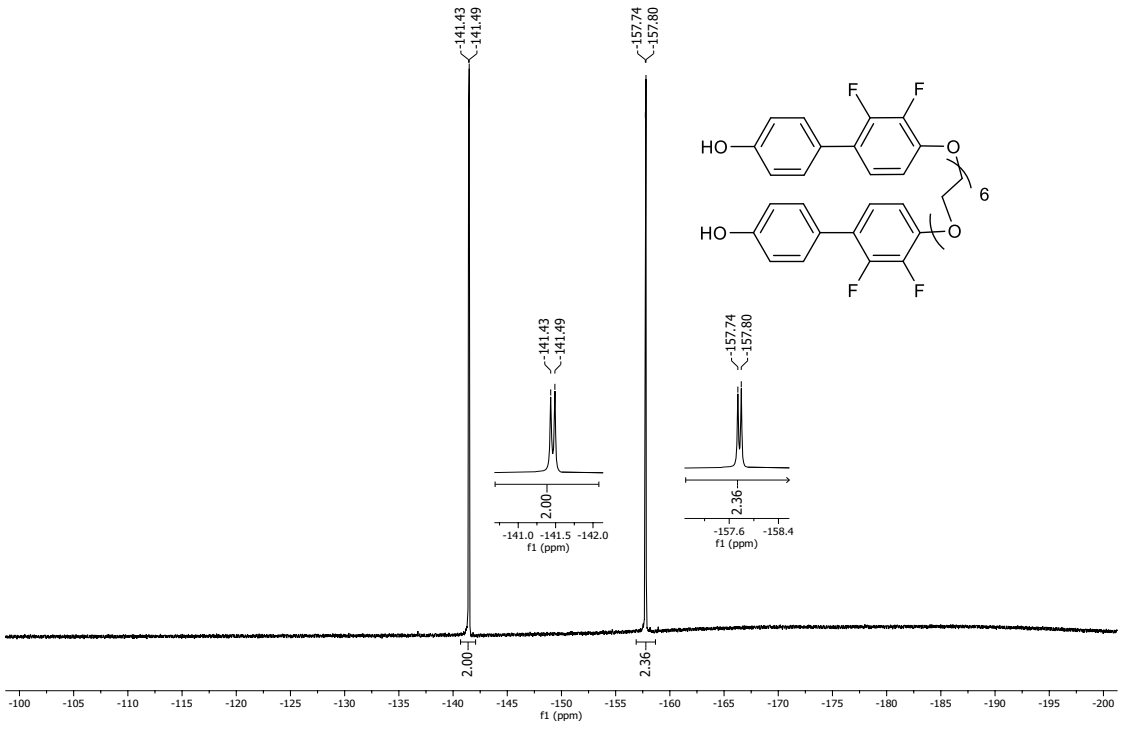

Figure S31. ^{19}F{^{1}H} NMR spectrum of **6[6]** (DMSO-d_6, 376 MHz).

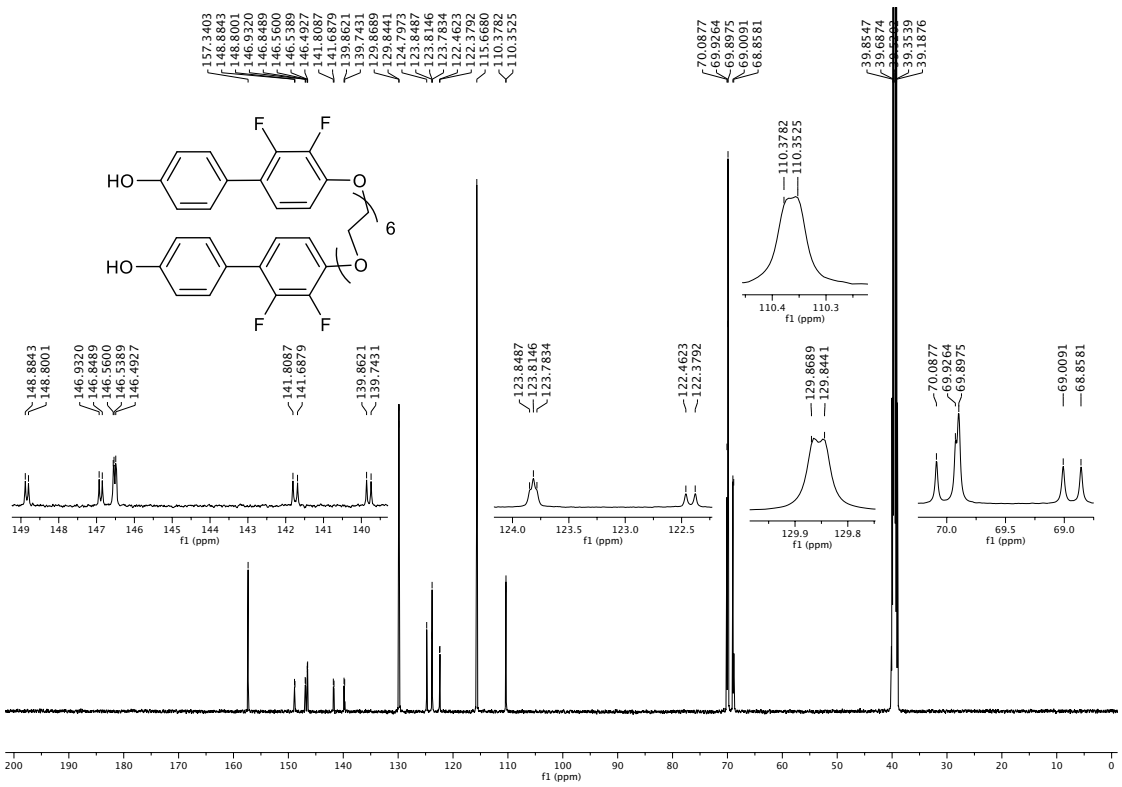

Figure S32. $^{13}C\{^{1}H\}$ NMR spectrum of **6[6]** (DMSO-d_6, 126 MHz).

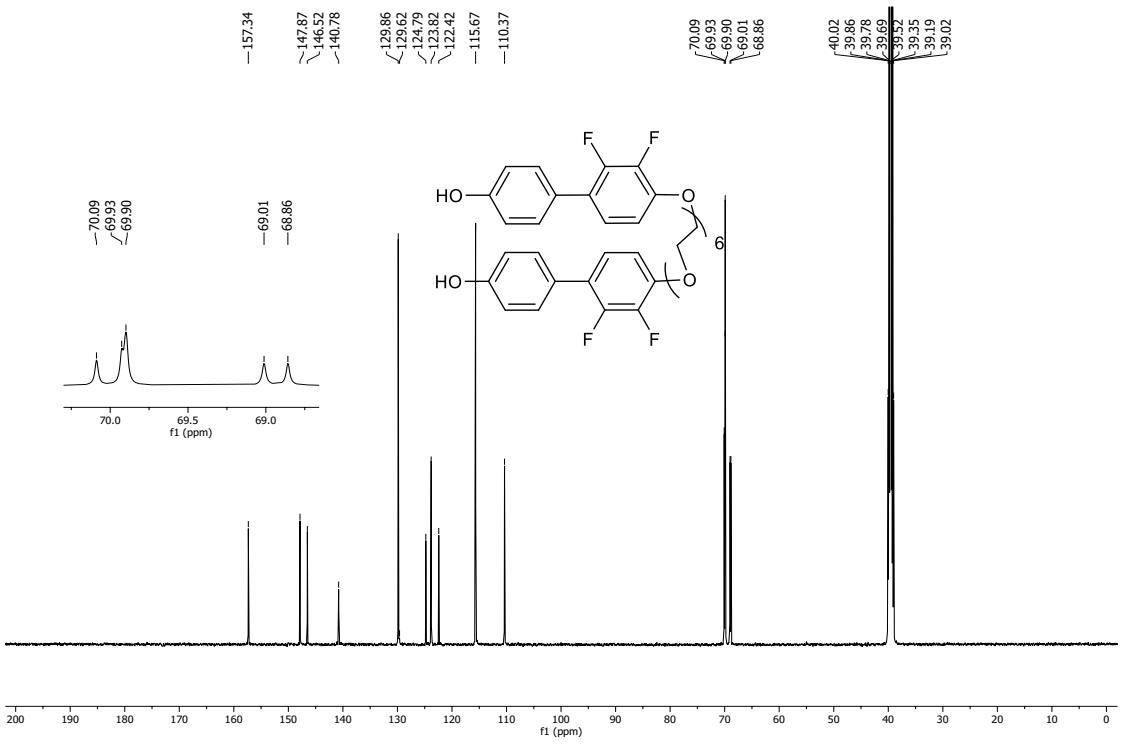

Figure S33. $^{13}C\{^{1}H;^{19}F\}$ NMR spectrum of **6[6]** (DMSO-d_6, 126 MHz).

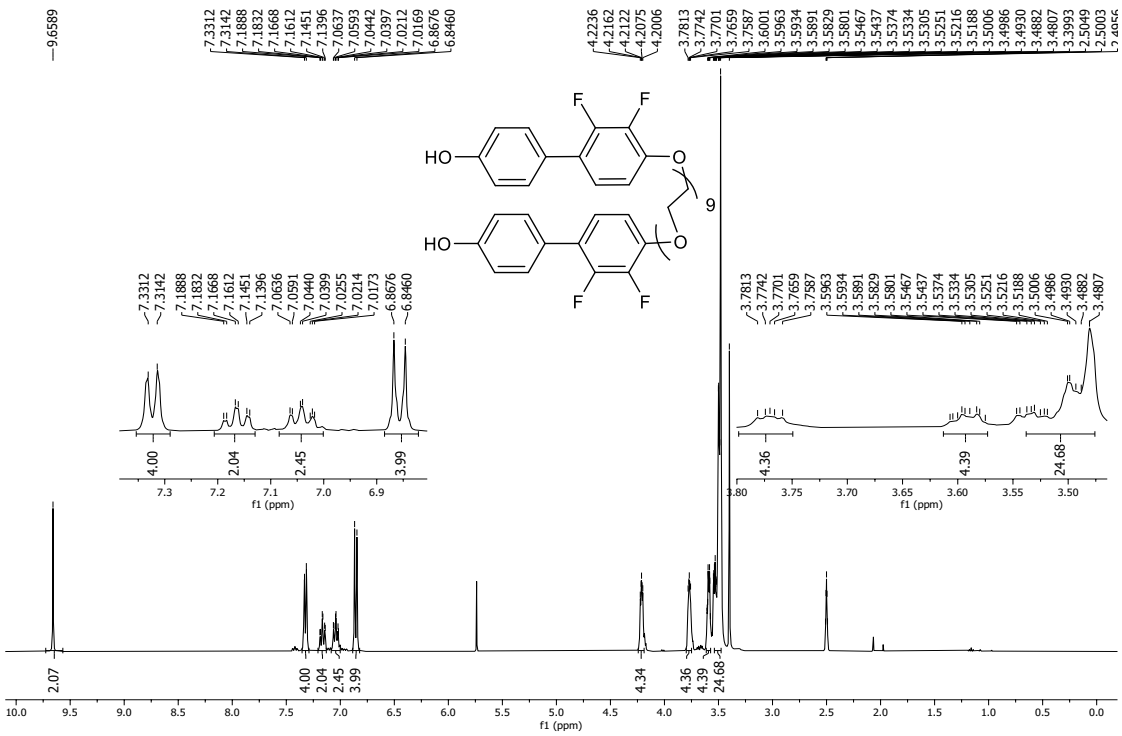

Figure S34. ^{1}H NMR spectrum of **6[9]** (DMSO-d_6, 400 MHz).

Figure S35. ^{19}F{^{1}H} NMR spectrum of **6[9]** ($CDCl_3$, 376 MHz).

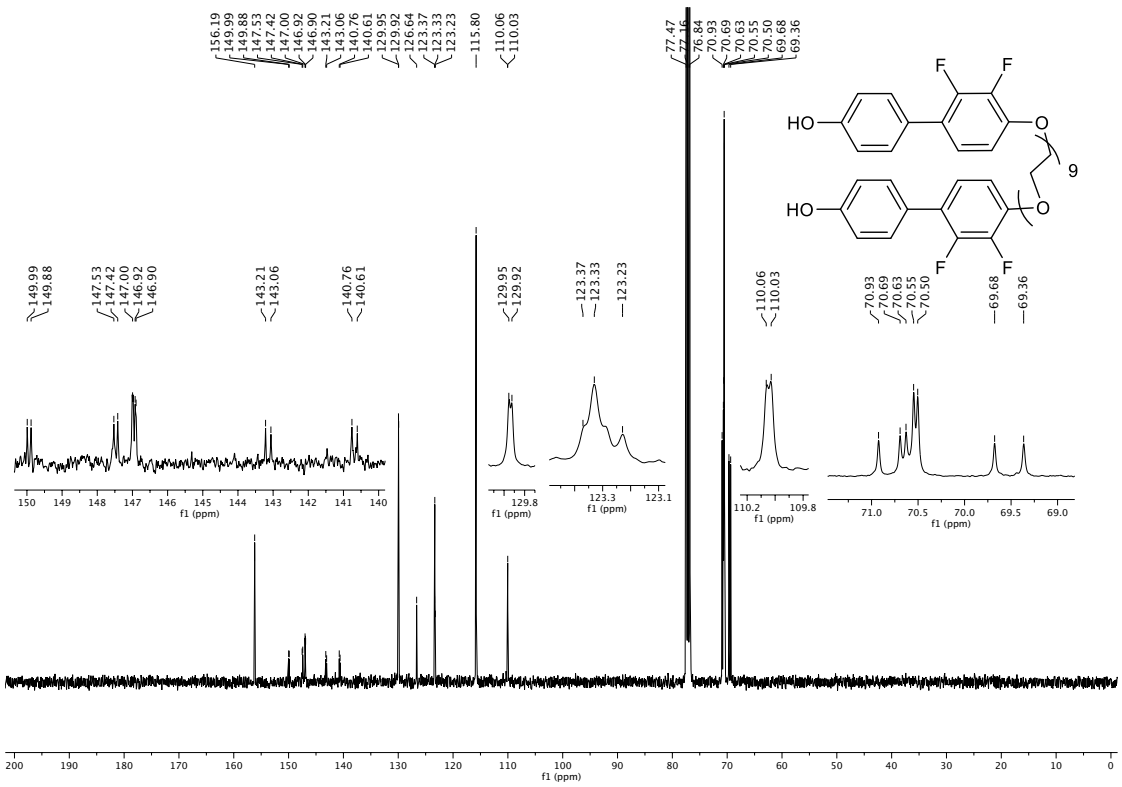

Figure S36. $^{13}C\{^{1}H\}$ NMR spectrum of **6[9]** ($CDCl_3$, 101 MHz).

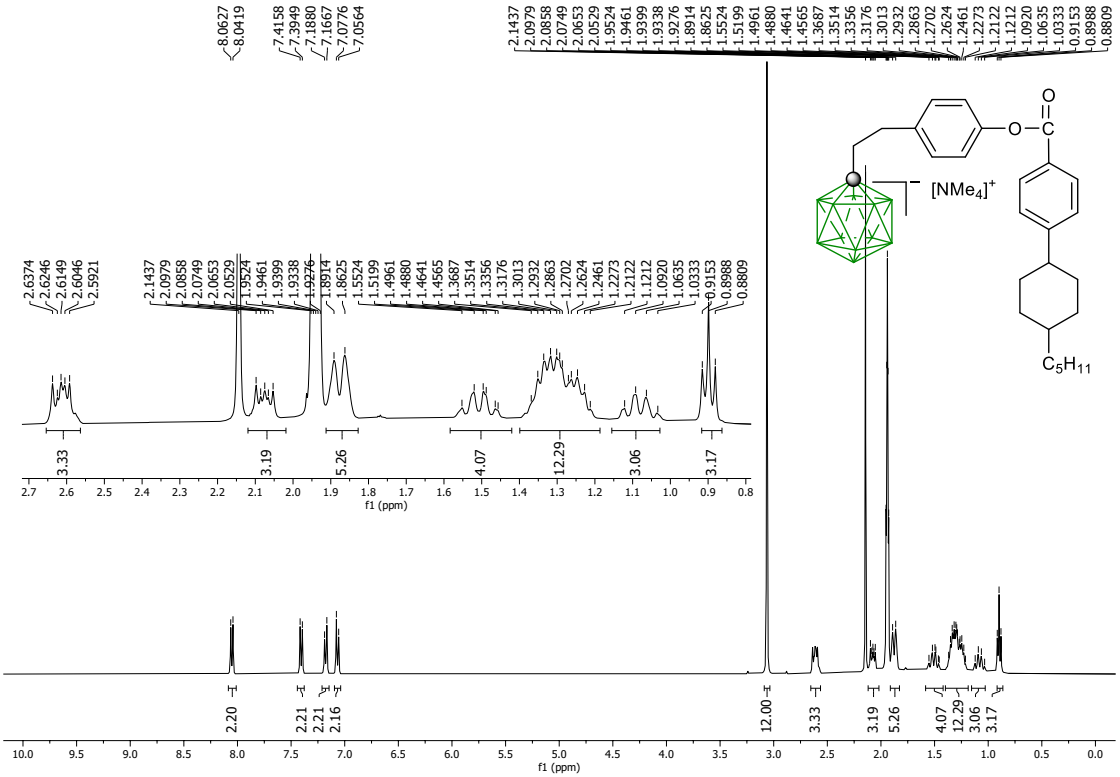

Figure S37. ^{1}H NMR spectrum of **S2[NMe$_4$]** (CD_3CN, 400 MHz).

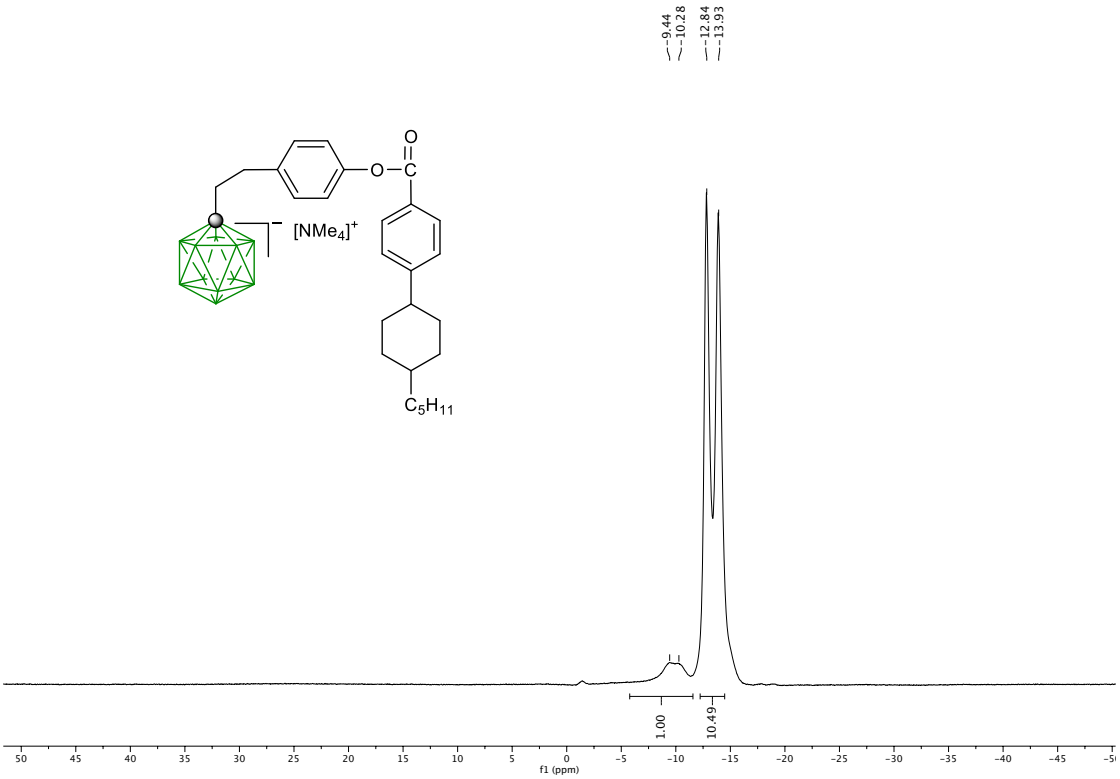

Figure S38. ^{11}B NMR spectrum of **S2[NMe$_4$]** (CD_3CN, 128 MHz).

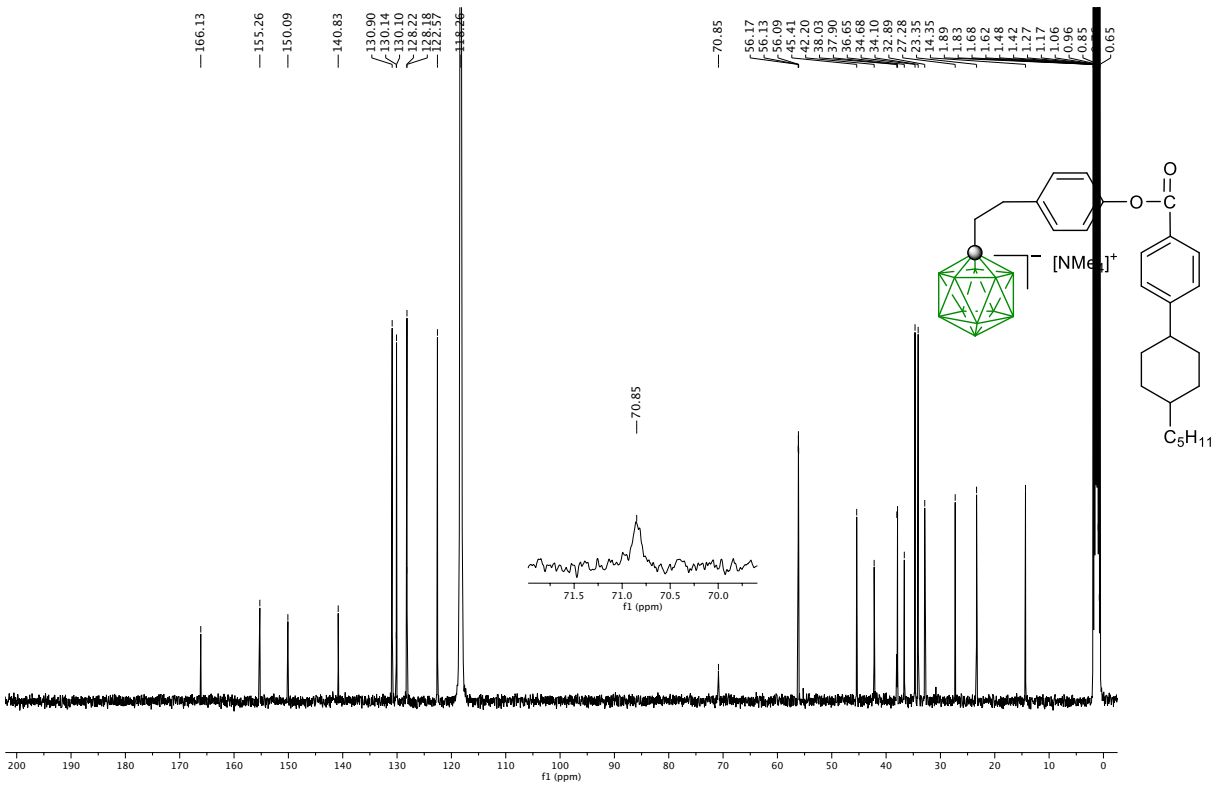

Figure S39. $^{13}C\{^{1}H\}$ NMR spectrum of **S2[NMe$_4$]** (CD_3CN, 101 MHz).

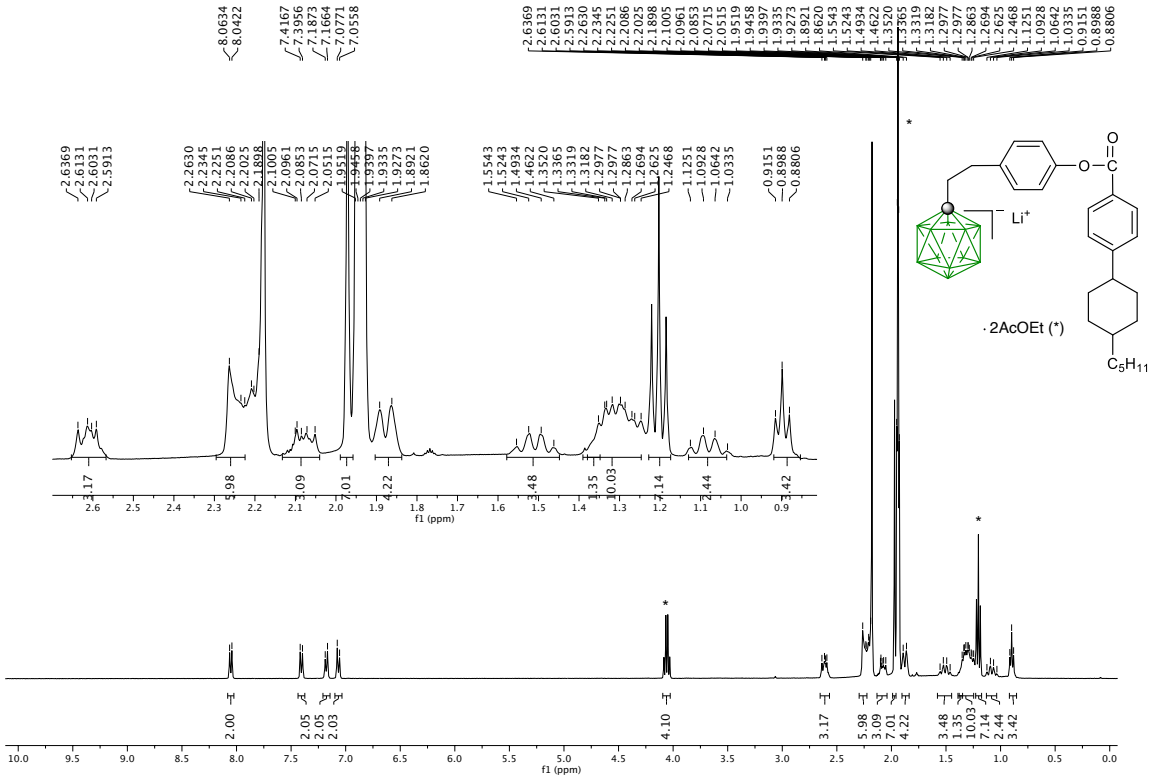

Figure S40. ^{1}H NMR spectrum of **S2[Li]** (CD_3CN, 400 MHz).

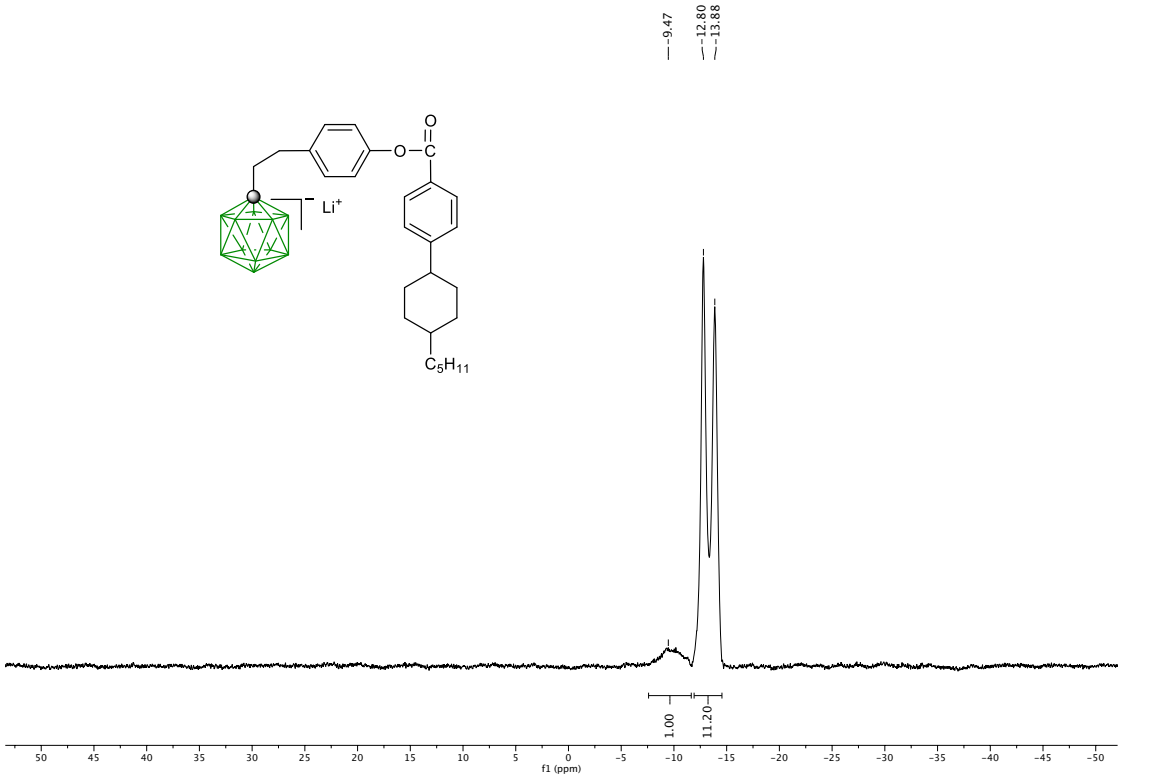

Figure S41. ^{11}B NMR spectrum of **S2[Li]** (CD_3CN, 128 MHz).

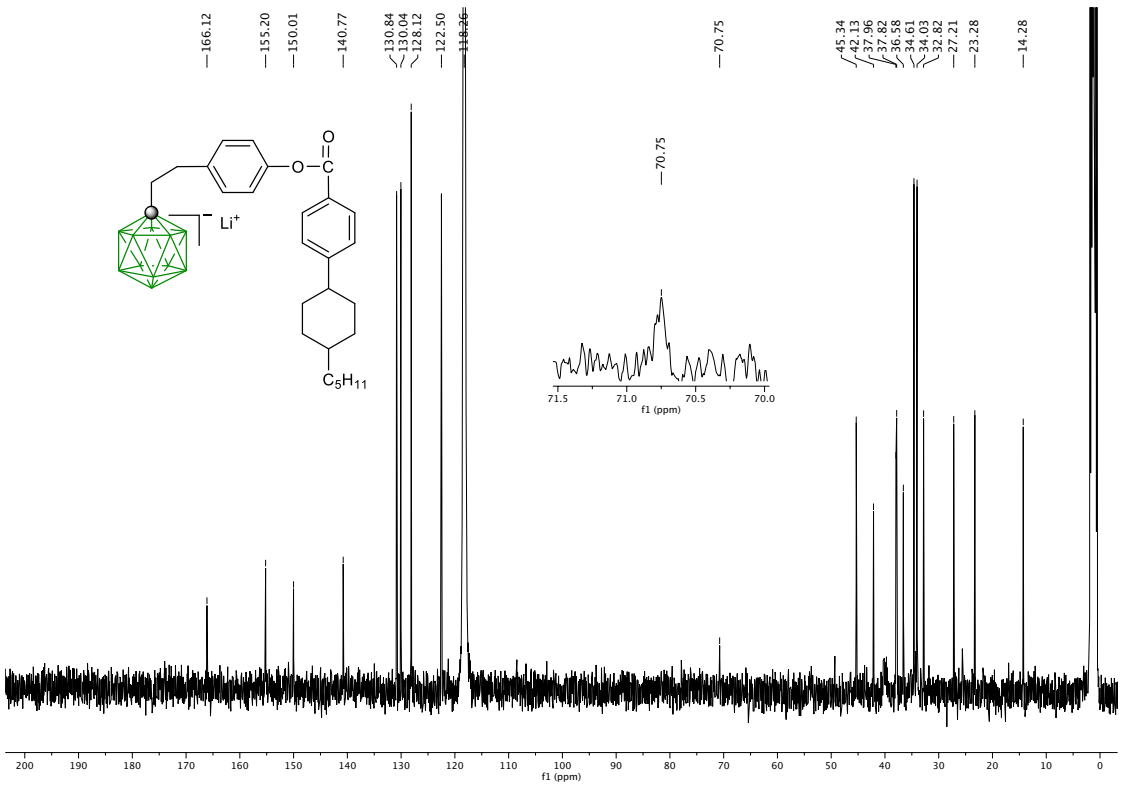

Figure S42. $^{13}C\{^{1}H\}$ NMR spectrum of **S2[Li]** (CD_3CN, 101 MHz).

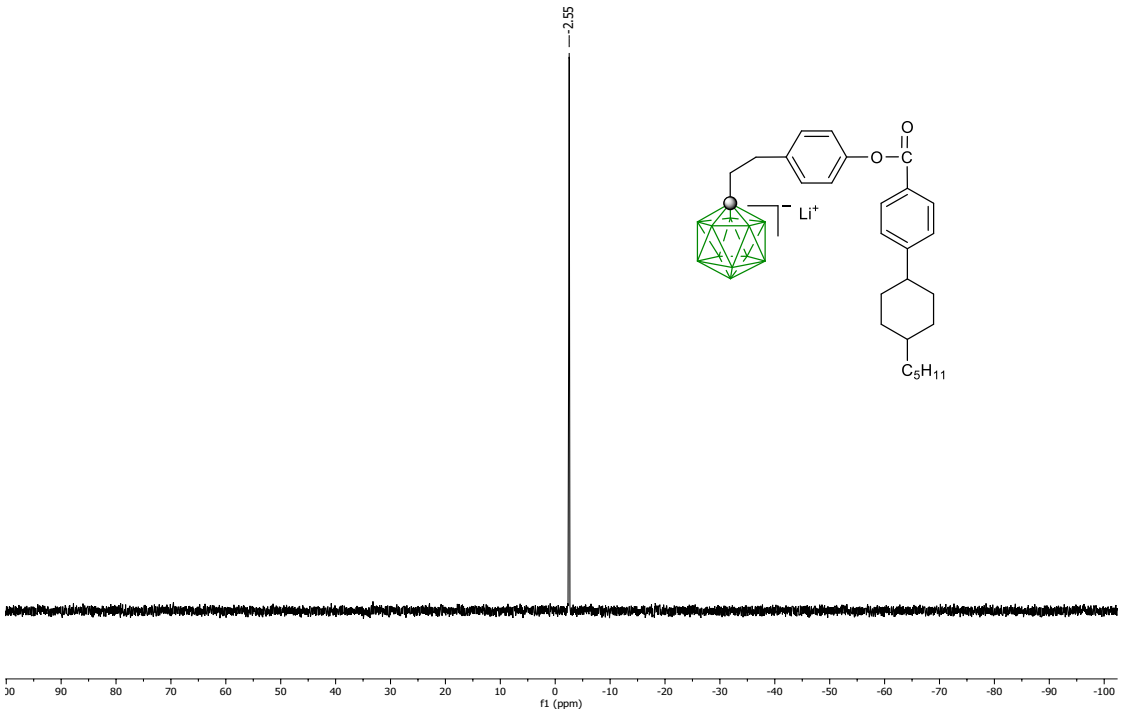

Figure S43. ^{7}Li NMR spectrum of **S2[Li]** ($CDCl_3$, 156MHz).

3. DSC measurements

DSC data were obtained with a DSC-2500 instrument and are shown in Figures S44–S48. Heating and cooling rates were 10 K min^{-1}.

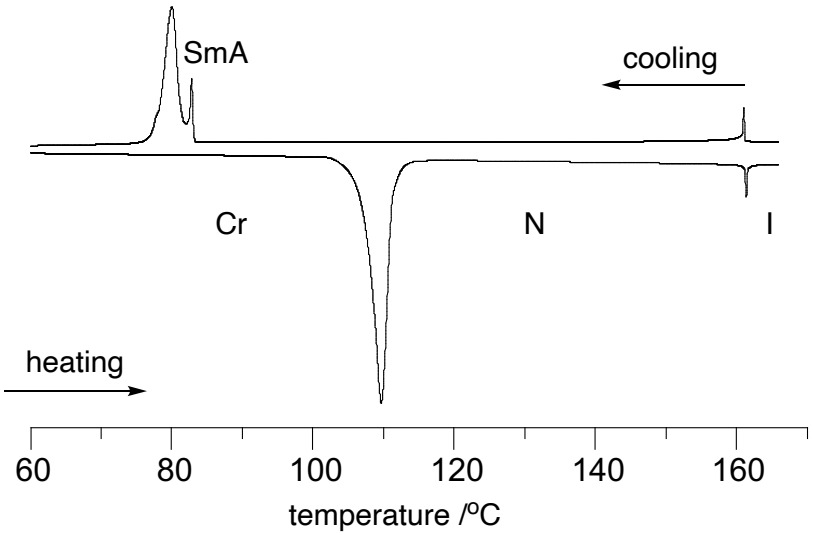

Figure S44. DSC trace of **2F[4]**.

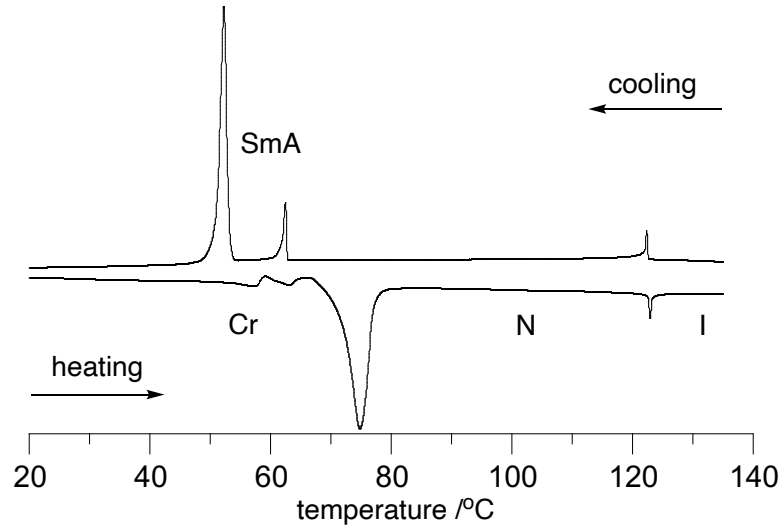

Figure S45. DSC trace of **2F[6]**.

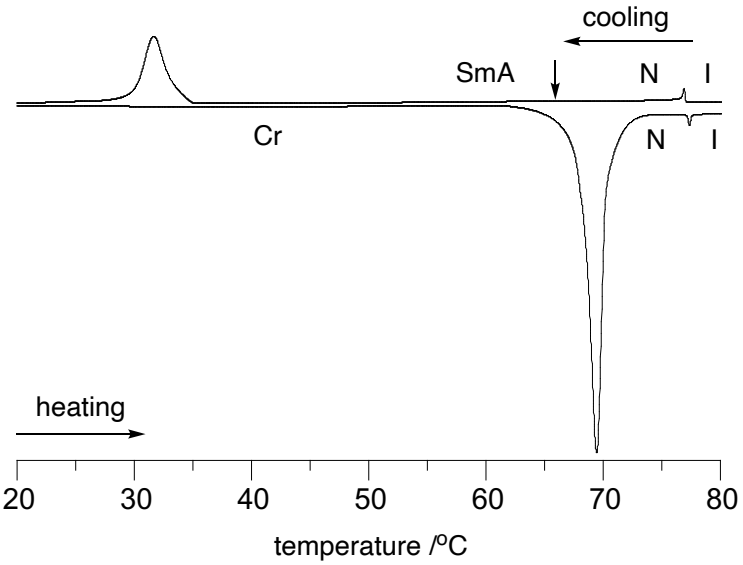

Figure S46. DSC trace of **2F[9]**.

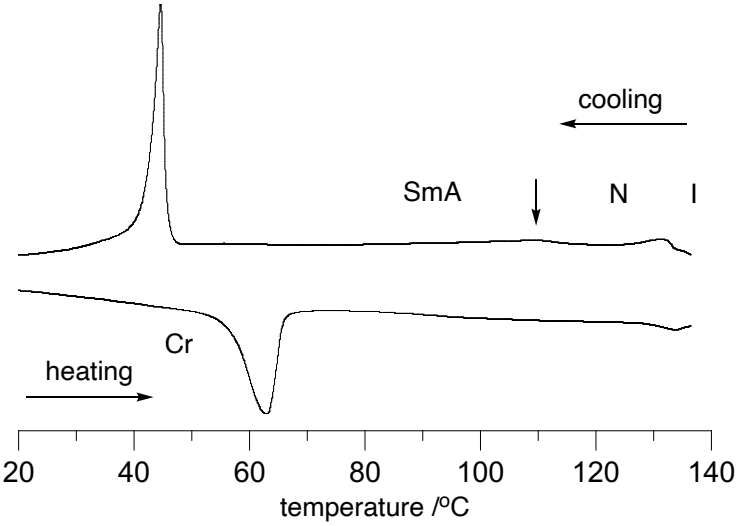

Figure S47. DSC trace of the electrolyte sample **2F[6]-S2[Li]**.

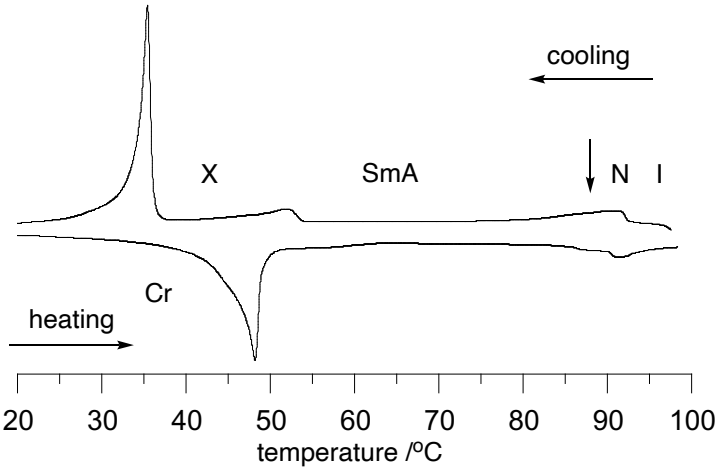

Figure S48. DSC trace of the electrolyte sample **2F[9]-S2[Li]**.

4. Additional photomicrographs of LC textures

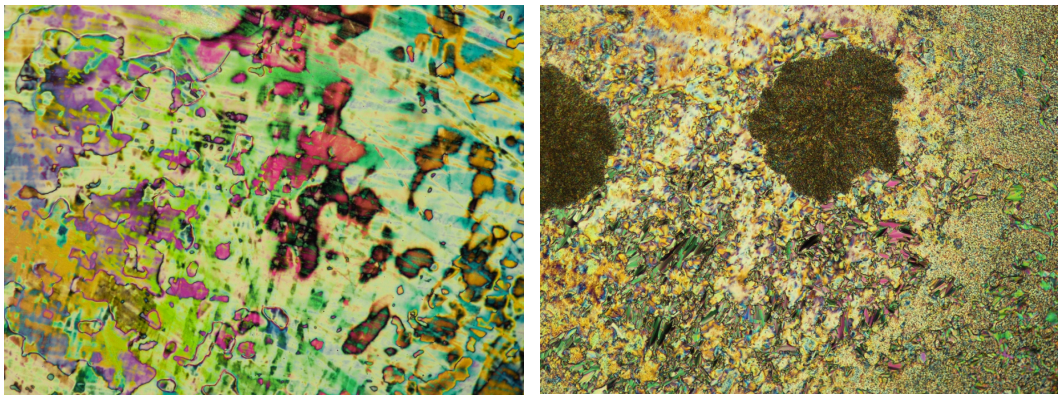

Figure S49. Photomicrographs of textures for 2F[4] obtained on cooling from the isotropic phase. Left: nematic phase at 151 ºC. Right: monotropic SmA phase and crystals growing from the nematic phase at 86 ºC.

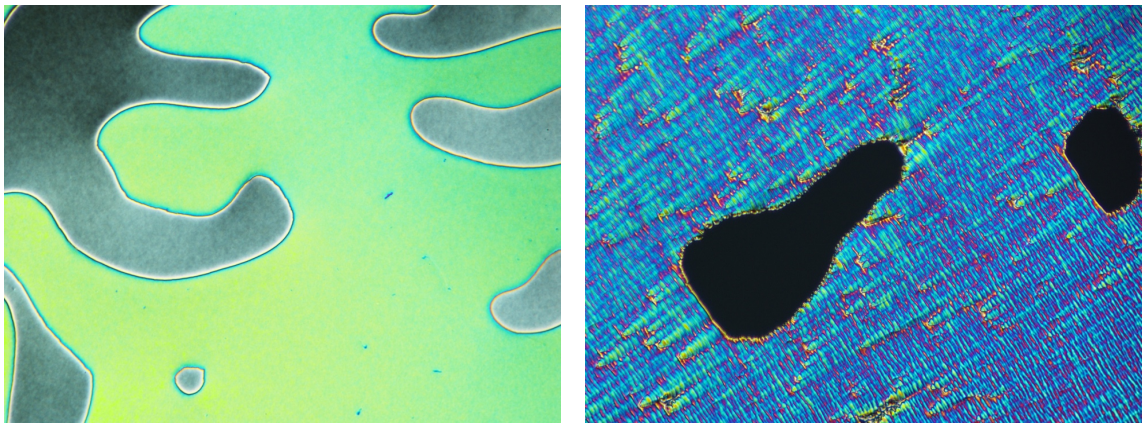

Figure S50. Photomicrographs of textures for **2F[9]** obtained on cooling from the isotropic phase. Left: nematic phase at 76 ºC. Right: monotropic SmA phase at 66 ºC.

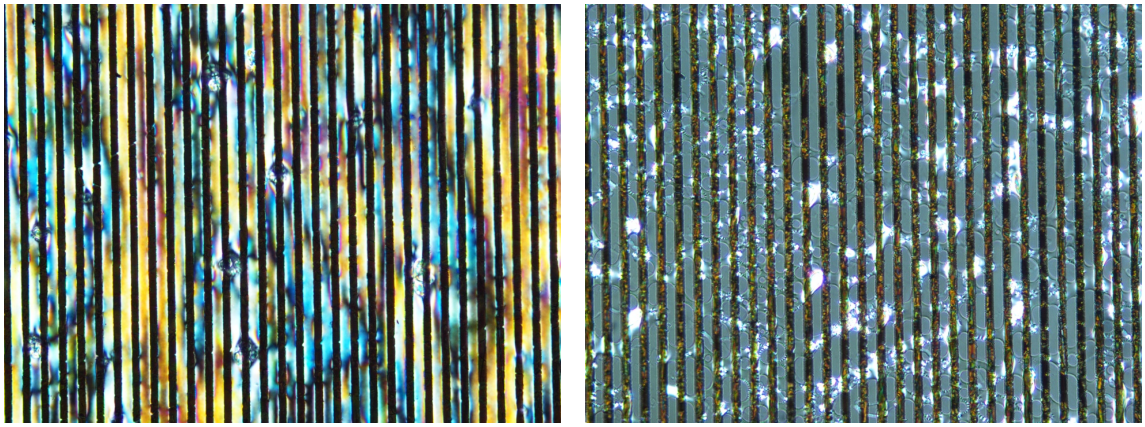

Figure S51. Photomicrographs of **2F[6]-S2[Li]** in a gold interdigitated electrode: nematic at 120 ºC (left) and SmA phase at 100 ºC (right).

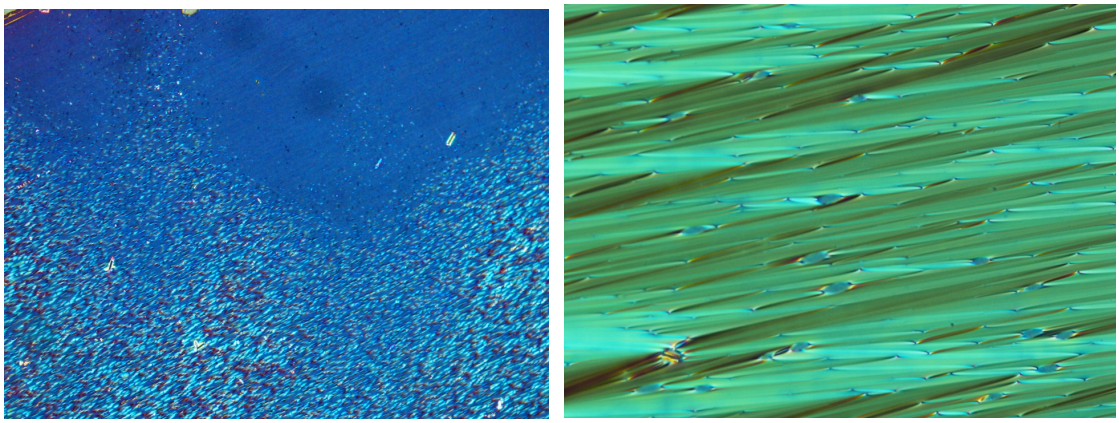

Figure S52. Photomicrographs of **2F[6]-S2[Li]** in an ITO cell with planar alignment: nematic at 120 ºC (left) and SmA phase at 115 ºC (right).

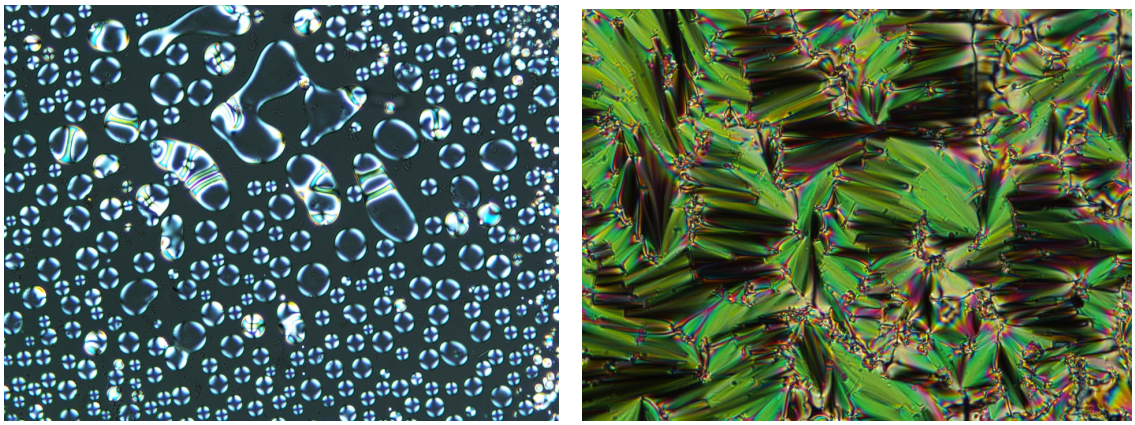

Figure S53. Photomicrographs of **2F[9]-S2[Li]**: nematic growing from the isotropic phase at 94 ºC (left) and SmA phase at 86 ºC (right).

5. Powder XRD data

Broad angle X-ray diffraction studies were performed for unaligned samples using a Bruker D8 GADDS instrument (Cu Kα radiation, λ=1.54 Å, incident beam formed by Göbel mirror monochromator and point collimator 0.5 mm, two-dimensional detector Vantec 2000). Samples were prepared in a form of a droplet on a heated surface; their temperature was controlled with a modified Linkam heating stage. Results are shown in the main text.

6. Sample preparation for EIS measurements

- **Interdigitated gold electrode**

The interdigitated gold electrode (gaps 10 μm between the electrodes) was purchased from Metrohm Dropsens (Figure S54).

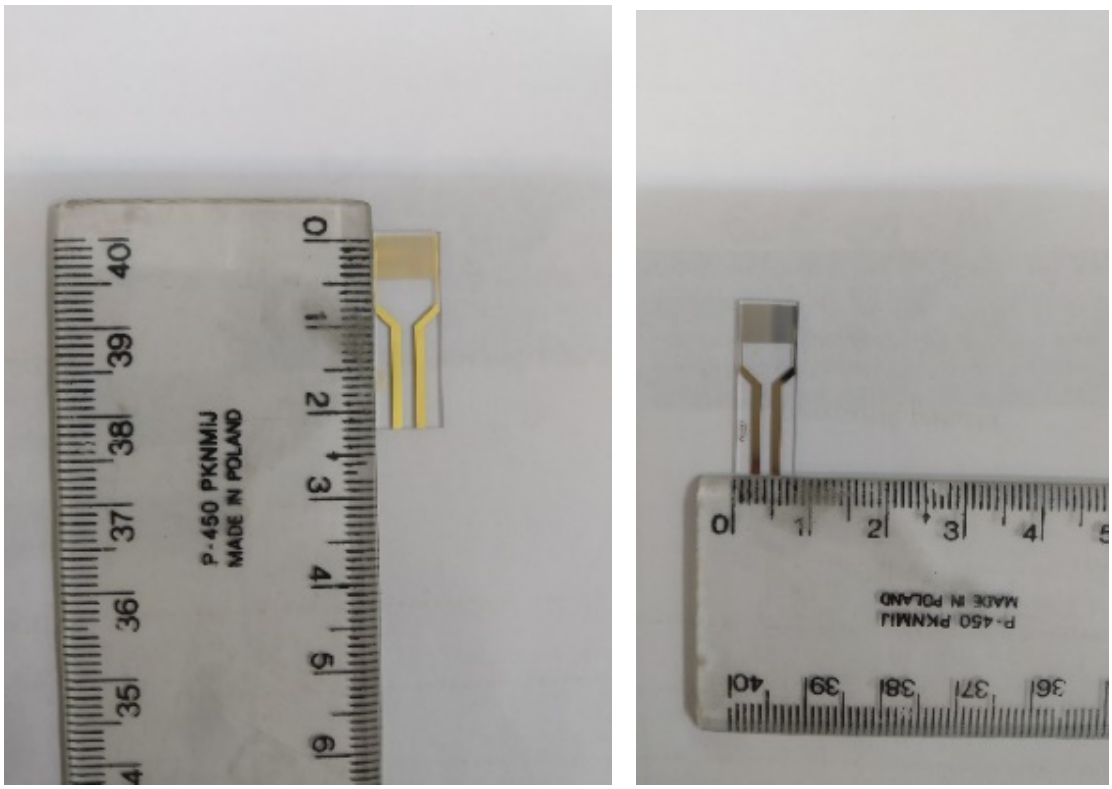

Figure S54. Interdigitated gold electrode.

The electrode surface was cleaned properly by wiping it with EtOH, and the electrolyte sample was deposited on the electrode surface. Then the cell was heated to the smectic phase temperature of the sample, and a glass plate was placed on top of the electrolyte sample and gently pressed on the top of the glass plate to fill the electrolyte sample on the electrode surface. Using a polarized optical microscope, the parallel alignment of the sample in the smectic phase was confirmed by heating the sample to the isotropic temperature and then cooling it to the smectic phase (for images see **2F[6]-S2[Li]** in the folder POM images). Copper wires were soldered to the cells in order to establish a proper connection for the EIS measurements (Figure S55).

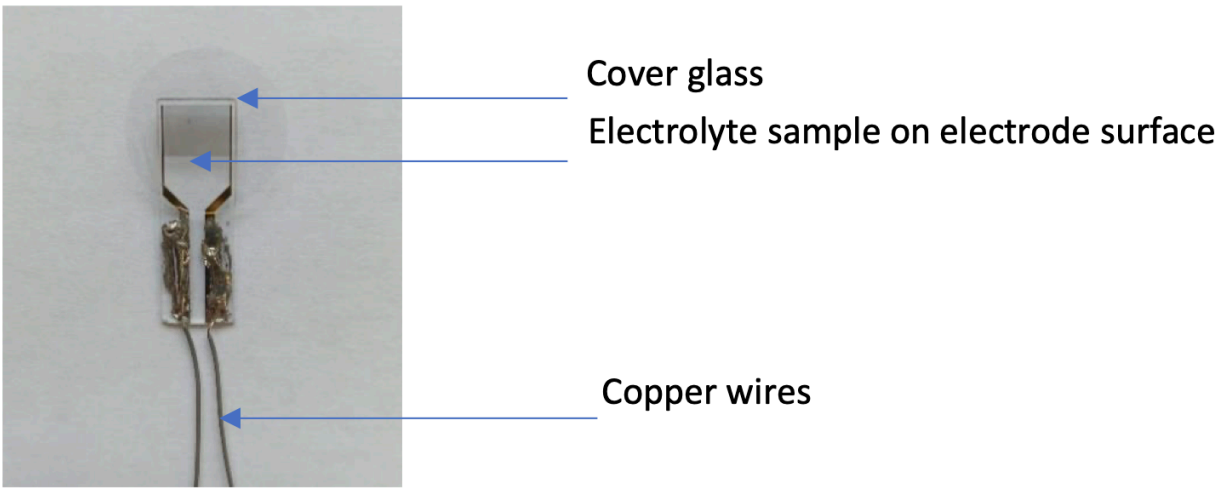

Figure S55. Interdigitated gold electrode containing the electrolyte sample.

- **ITO cell**

HG cells (homogeneous cells for parallel alignment of the sample) with different cell thicknesses and alignment layers were used. HG cells coated with polyimides gave only a partial alignment of the sample, while HG cells coated with nylon 6 having a 10 µm provided good parallel alignment of the sample. Therefore, nylon 6-coated cells with 10 µm thickness were used for preparing a parallelly aligned electrolyte sample for the ionic conductivity studies (Figure S56).

The ITO cells were filled with the electrolyte samples at their isotropic temperature by capillary flow. Then, the sample was cooled down slowly (2 K/min) to the smectic phase temperature range using a hot stage, and the alignment of the sample was studied using a polarized optical microscope (POM) to confirm parallel alignment of the sample inside the cells (for images see **2F[6]-S2[Li]** above).

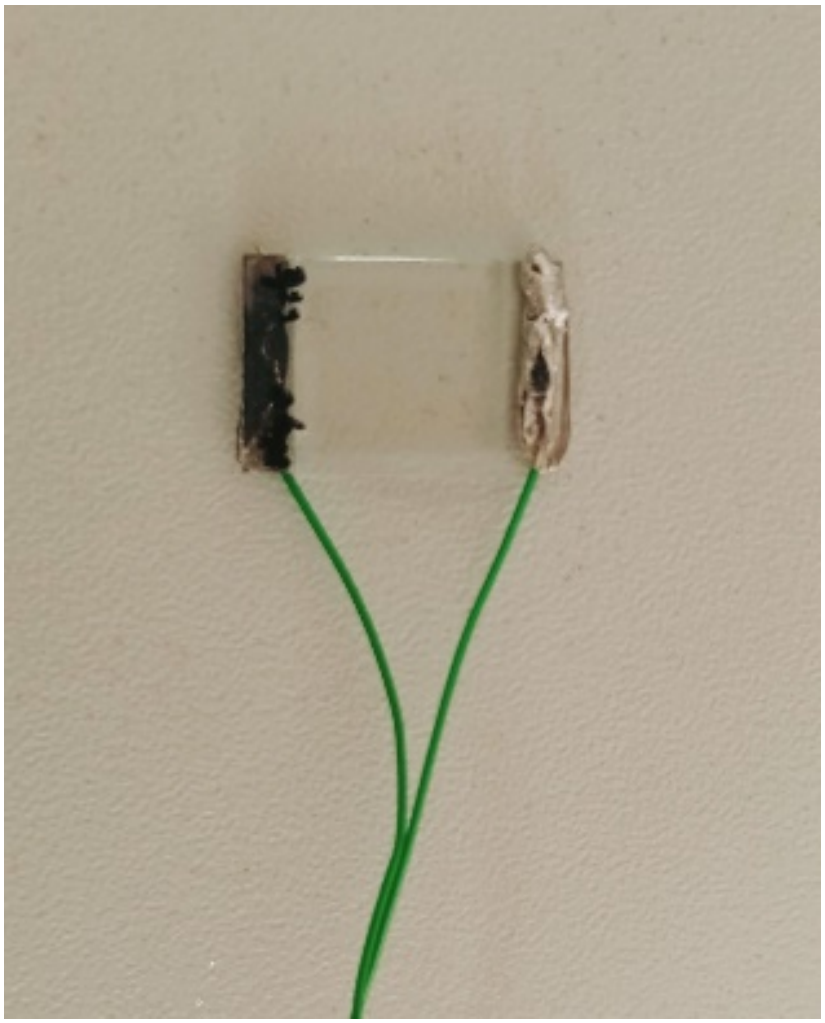

Figure S56. ITO cell connected with copper wires.

7. EIS measurements

Electrochemical impedance spectroscopy measurements were performed in the range of 60 to 140 °C using two types of cells for measuring the ionic conductivity in the parallel and perpendicular directions relative to the smectic layer (interdigitated gold electrode and ITO cell, respectively). A computer-interfaced multichannel potentiostat with a frequency range of 500 kHz to 1 Hz and a 5 mV AC signal amplitude was used for the electrochemical impedance spectroscopy measurements. Two types of cells were used for measuring the ionic conductivity in the parallel and perpendicular directions (interdigitated gold electrode and ITO cell, respectively). Cells were filled with the electrolytes in their respective isotropic phases. At

each temperature point the cells were thermostated for a minimum of one hour using a cryostat-thermostat system (Haake K75 with a DC50 temperature controller), before taking a series of measurements, which were averaged. The obtained data are shown in Tables S1 and S2, while Arrhenius plots of the data are presented in Figures S57–S58.

Table S1. Data for anisotropic conductivity for the system **2F[6]-S2[Li]**.

Temperature /^{o}C	$\sigma_{\perp}$ /mS cm^{-1}	$\sigma_{\parallel}$ /mS cm^{-1}
40	0.00035	0.00018
60	0.00123	0.00345
70	0.00517	0.01383
80	0.01028	0.02139
90	0.01962	0.03007
100	0.03695	0.03675
110	0.06443	0.04374
120	0.09361	0.05131
125		0.02590
130	0.08382	
135		0.03413
140	0.11132	0.03839

Table S2. Data for anisotropic conductivity for the system **2F[9]-S2[Li]**.

Temperature /°C	$\sigma_{\perp}$ /mS cm^{-1}	$\sigma_{\parallel}$ /mS cm^{-1}
60	0.00399	0.00066
65	0.01299	0.00431
70	0.01772	0.00611
75	0.02022	0.00752
80	0.02743	0.00907
85	0.03540	0.01284
90	0.05261	0.01569
95	0.06675	0.01799

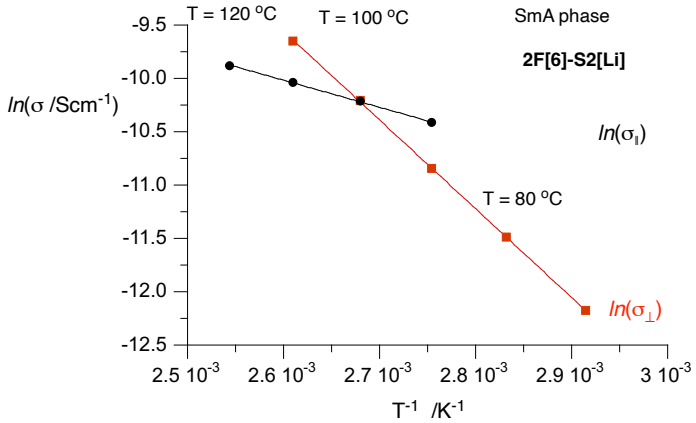

Figure S57. Temperature dependent ionic conductivity in the electrolyte sample **2F[6]-S2[Li]** in the parallel and perpendicular directions. Best fitting lines:
$ln(\sigma_{\perp}) = -8323(47)\times 1/T + 12.1(1)$, $r^2 = 0.999$;
$ln(\sigma_{\parallel}) = -2540(52)\times 1/T - 3.4(1)$, $r^2 = 0.999$.

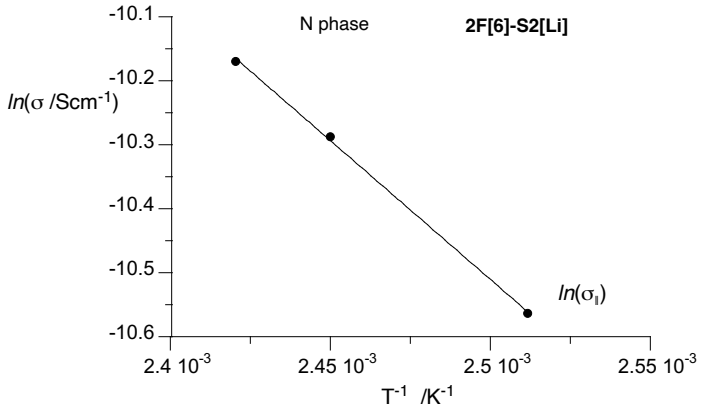

Figure S58. Temperature dependent ionic conductivity of the electrolyte sample **2F[6]-S2[Li]** in the parallel direction in the nematic phase. Best fitting line:
$ln(\sigma_{\parallel}) = -4341(122)\times 1/T + 0.34(30)$, $r^2 = 0.999$.

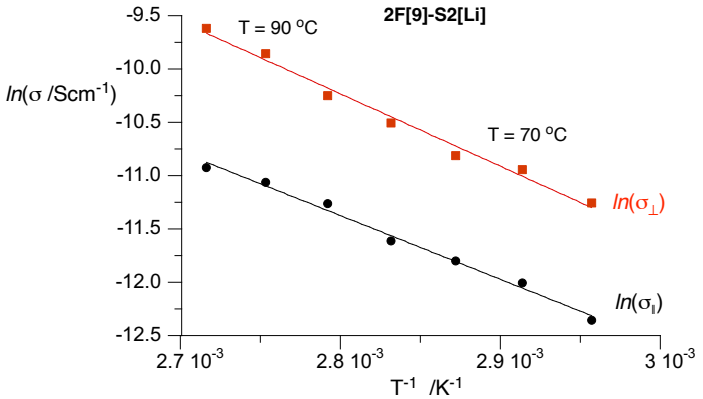

Figure S59. Temperature dependent ionic conductivity in the electrolyte sample **2F[9]-S2[Li]** in the parallel and perpendicular direction in the SmA phase. Best fitting lines:
$ln(\sigma_{\perp}) = -6789(359)\times 1/T + 8.8(10)$, $r^2 = 0.986$;
$ln(\sigma_{\parallel}) = -5974(252)\times 1/T + 5.5(7)$, $r^2 = 0.991$.

8. Computational details

Geometry optimization for anion **S2** and host half molecules were carried out with the B3LYP[3,4] method and 6-31(d) basis sets[5,6] using Gaussian 09 package[7] in vacuum and default convergence limits. The alkyl and oligoethylene oxide chains were initially set at most extended *trans* conformation. Optimized geometries are shown in Figure S60.

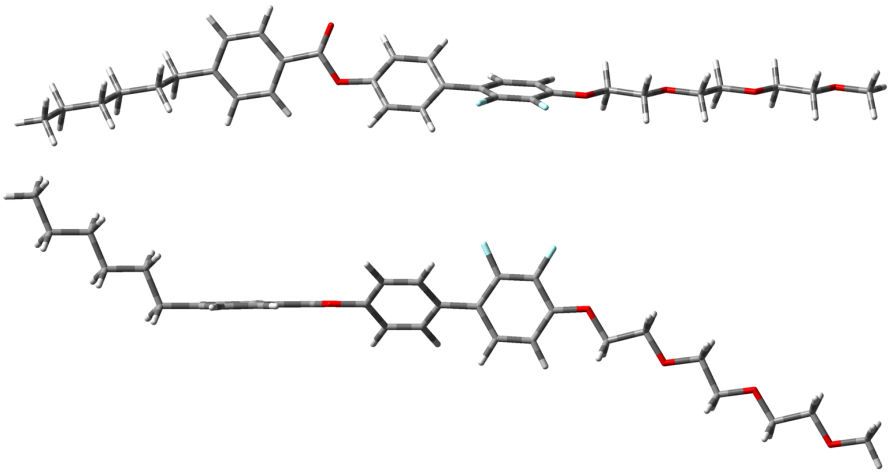

Half molecule 2F[6]

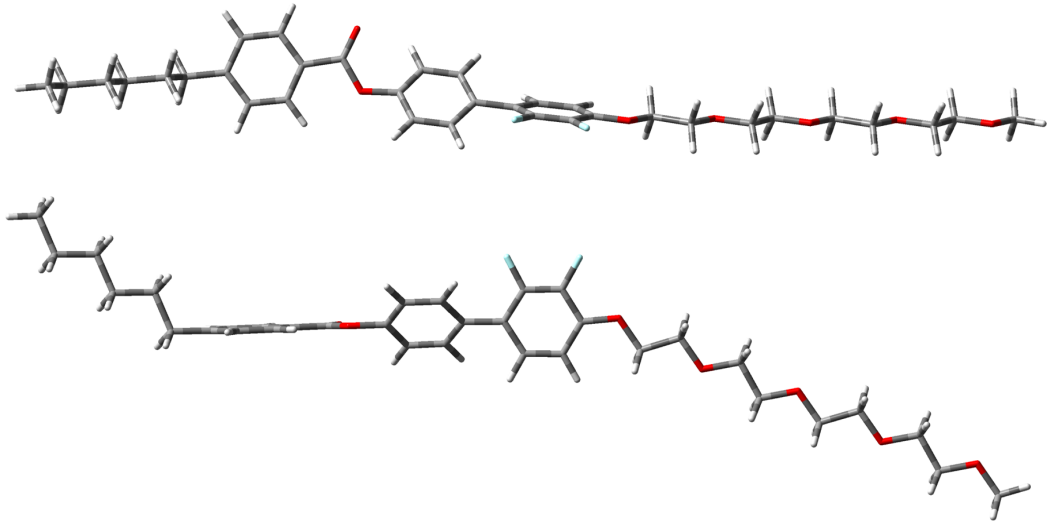

Half molecule 2F[9]

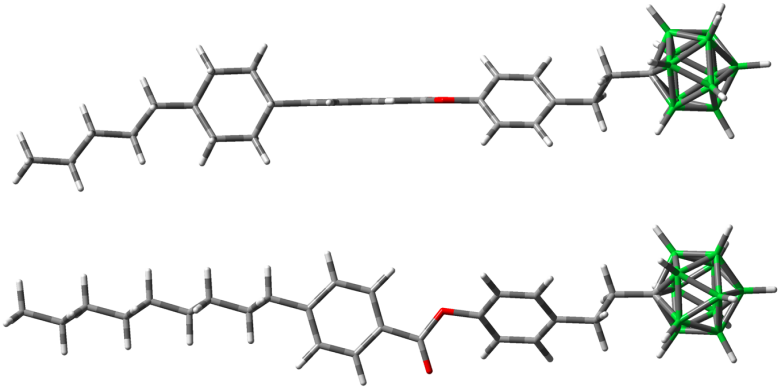

Anion **S2**

Figure S60 Two views of DFT optimized molecule corresponding to half molecule of host **2F[6]** and **2F[9]** and the anion **S2** in vacuum.

2F[6] half molecule

1\1\GINC-GAUSIANDELL\FOpt\RB3LYP\6-31G(d)\C32H38F2O6\PKASZYNSKI\18-Mar
-2024\0\\#P B3LYP/6-31G(d) fopt geom=(nodistance,noangle) scf=direct\\
C6PhCOO-PhPhF2-O(CH2CH2O)3-Me, half of the 2F[6]host\\0,1\C,-8.6177677
332,1.8419122353,-2.7060904218\C,-9.1976734931,1.5048840829,-1.4737841
992\C,-8.3481189853,1.2788238024,-0.3805562852\C,-6.9661193926,1.38447
05845,-0.5067409213\C,-6.3990206879,1.7196681308,-1.7446915097\C,-7.23
81861288,1.9479095453,-2.8443537495\H,-8.7780418747,1.0100222598,0.581
7428951\H,-6.7888875439,2.2014035413,-3.7989916993\H,-6.3234719398,1.2
01853323,0.3469858029\H,-9.2585574727,2.0156488165,-3.5675575383\C,-10
.6995183404,1.4211287766,-1.3187471899\C,-11.3345342084,2.7491399989,-
0.8554082195\H,-10.951450949,0.6347509283,-0.5948616676\H,-11.15132504
57,1.1235076219,-2.2740038835\H,-10.8830407435,3.0490137884,0.10050727
76\H,-11.0789602034,3.5400057424,-1.574100032\C,-12.858008444,2.660884
5312,-0.7027991943\C,-13.5015823633,3.9707163872,-0.2300162868\H,-13.1
057367067,1.8574213191,0.0068585012\H,-13.3024837993,2.3634553956,-1.6
642504657\C,-15.0260960123,3.8834166743,-0.0810641988\H,-13.0596851821
,4.2663587944,0.7331966086\H,-13.2521716629,4.7755791512,-0.9373459539
\C,-15.6626106405,5.1928456702,0.3958638175\H,-15.4674388239,3.5910621
298,-1.0445287539\H,-15.2747811427,3.0770911626,0.6235732804\H,-16.750
2847204,5.0979470188,0.4911493668\H,-15.2673207779,5.4924556476,1.3743
341824\H,-15.4599271719,6.0110287744,-0.3062443825\C,-4.9331620443,1.8
328186787,-1.9579786168\O,-4.4043707594,2.0897599319,-3.016634371\O,-4
.2415441786,1.609616746,-0.7933372671\C,-2.8491706147,1.6369657369,-0.
7621752821\C,-2.2734048435,2.2897010232,0.3262358973\C,-2.052545607,0.
9820375798,-1.7008660896\C,-0.8905989947,2.2890880432,0.4825232778\H,-
2.9167060987,2.7853557239,1.046432595\C,-0.6696410067,0.9934265203,-1.
5352155271\H,-2.5007032937,0.4907379504,-2.5547513735\C,-0.0602530568,
1.6360076645,-0.4443732345\H,-0.45429463,2.7932876416,1.337139036\H,-0
.0493718776,0.5062980906,-2.2819419617\C,1.4132726997,1.584412019,-0.2
774875278\C,2.1460108165,0.4253232462,-0.5727975306\C,2.1584833333,2.6
857342772,0.1707675956\C,3.5327764392,0.3551623527,-0.435138669\H,1.60
85472358,-0.4596790903,-0.8981699199\C,3.537251375,2.6363853989,0.3163
150418\C,4.2513286469,1.4679223983,0.0139807771\H,4.0458578267,-0.5702
961437,-0.6679276683\F,1.5536996187,3.8529593732,0.4682916413\F,4.1949
363844,3.7264159533,0.7429516007\O,5.5958553917,1.5330272939,0.1974389
622\C,6.3678119037,0.3669215919,-0.072143741\C,7.8171261548,0.72437726
44,0.2232203072\H,6.2608208879,0.0622302536,-1.1213958963\H,6.04931548
69,-0.4670512136,0.5668358567\H,8.1351935948,1.5611894266,-0.418405644
2\H,7.9154264525,1.0497573504,1.2708868934\C,9.9670165217,-0.256029625
6,0.2083037125\H,10.3797861561,0.5310062245,-0.4422379241\H,10.1539626
053,0.0403177152,1.2524552537\C,10.6565125308,-1.5810451197,-0.0827704
078\H,10.4670054833,-1.8780193879,-1.1268555731\H,10.2406302861,-2.367
2956214,0.5676763214\C,12.8007529916,-2.5697262874,-0.0824544585\C,14.
256770185,-2.2365238117,0.2079232513\H,12.4712453758,-3.3955862496,0.5
679744677\H,12.6970274956,-2.905595105,-1.1265201745\H,14.5855467694,-
1.4085312981,-0.4416242121\H,14.3601835593,-1.899625979,1.2526209468\C
,16.3933371613,-3.2200298311,0.2082821187\H,16.8197485216,-2.442800639
4,-0.4463568175\H,16.5922453408,-2.937329654,1.2546873758\O,8.58215652
75,-0.4361683787,-0.0280565204\O,12.0381344153,-1.401036521,0.15377721
88\O,15.0146215424,-3.4048676658,-0.0298441492\H,16.8875624483,-4.1720
516021,-0.0024012506\\Version=ES64L-G09RevD.01\State=1-A\HF=-1893.2785
839\RMSD=6.573e-09\RMSF=1.647e-06\Dipole=-0.2674202,-1.0320413,0.42096
96\Quadrupole=42.4718716,-24.7482565,-17.7236151,-6.3153485,-1.1486505
,0.7276196\PG=C01 [X(C32H38F2O6)]\\

2F[9] half molecule

1\1\GINC-GAUSIANDELL\FOpt\RB3LYP\6-31G(d)\C34H42F2O7\PKASZYNSKI\18-Mar
-2024\0\\#P B3LYP/6-31G(d) fopt geom=(nodistance,noangle) scf=direct\\
C6PhCOO-PhPhF2-O(CH2CH2O)4-Me, half of the 2F[9]host\\0,1\C,8.71832347
32,-1.770595615,1.0075607113\C,9.2097670849,-1.4736736004,-0.273074309
2\C,8.3072680995,-0.9997287482,-1.2362713424\C,6.9593758096,-0.8219998
608,-0.9367442181\C,6.4817024851,-1.1198011563,0.3473067783\C,7.374414
4273,-1.5972110979,1.3177133454\H,8.6673047403,-0.7705909885,-2.236725
8393\H,6.9933506466,-1.829931931,2.3066690764\H,6.27432509,-0.45763263
44,-1.6937868632\H,9.4003741614,-2.1463955468,1.7668867861\C,10.680726
8571,-1.62156481,-0.5908444471\C,11.4992083941,-0.3621970199,-0.235940
7988\H,10.8077698951,-1.8421526991,-1.6586988087\H,11.0914643735,-2.47
94906283,-0.0421983085\H,11.0923651067,0.4969141221,-0.7872187075\H,11
.359797348,-0.1333860774,0.829759556\C,12.9947167696,-0.5122229104,-0.
5404512503\C,13.8158774734,0.7334152354,-0.1829027044\H,13.1280161819,
-0.7418717972,-1.6081021125\H,13.3919595868,-1.3791961891,0.0081833749
\C,15.3136408989,0.5863813756,-0.4809218486\H,13.4201756319,1.60028052
21,-0.7327665894\H,13.6798679462,0.9639858567,0.8842015898\C,16.126305
2006,1.833416764,-0.1178369875\H,15.7083939041,-0.280538842,0.06786057
44\H,15.4500322345,0.3580691798,-1.5476392124\H,17.1900889362,1.698087
0309,-0.3440765514\H,15.7761325593,2.7109349903,-0.6752821492\H,16.039
9280788,2.065534572,0.9508138644\C,5.0574414763,-0.9598631587,0.738577
4033\O,4.6082760566,-1.2151479835,1.8340574775\O,4.3054059644,-0.47889
6151,-0.3036632447\C,2.93771426,-0.2495225727,-0.173557529\C,2.4544290
547,0.9016303281,-0.7938106764\C,2.0646437304,-1.1365637421,0.45600275
83\C,1.0900229254,1.1739167278,-0.7855120109\H,3.1542237352,1.57073573
25,-1.2845209426\C,0.7018092953,-0.8481379846,0.4621545033\H,2.4419926
352,-2.0211435466,0.951353109\C,0.1841544049,0.3014161857,-0.157913511
8\H,0.7262095815,2.0686811753,-1.277222542\H,0.027828741,-1.5245785965
,0.9795352636\C,-1.2786232768,0.5504070882,-0.1628731014\C,-2.20226534
14,-0.4947973655,-0.3124885996\C,-1.8239204345,1.8336578722,-0.0031406
322\C,-3.5822440323,-0.2886103337,-0.3022463247\H,-1.8268500113,-1.501
451821,-0.46614613\C,-3.1924708116,2.0607226134,0.0068366828\C,-4.0989
371614,1.0008748751,-0.1395781799\H,-4.2485031974,-1.132970529,-0.4325
771224\F,-1.0261198664,2.9071139249,0.1642293458\F,-3.6519032702,3.311
4878887,0.1719325791\O,-5.4140529494,1.3405035479,-0.1144380379\C,-6.3
799650924,0.3018220428,-0.2431824653\C,-7.7466247578,0.9652596625,-0.1
559150925\H,-6.267878856,-0.4366251974,0.5613918738\H,-6.272302132,-0.
2137132767,-1.2064982199\H,-7.8451594944,1.4924630302,0.8060517691\H,-
7.8521909932,1.7117329075,-0.9589003805\C,-10.0420214186,0.4108770953,
-0.2164858028\H,-10.2350562581,0.9215456146,0.7400533436\H,-10.2450122
908,1.1292071812,-1.0263319329\C,-10.9617950996,-0.7936832224,-0.35265
80345\H,-10.7575359769,-1.5115152792,0.4580138599\H,-10.7659500606,-1.
3060621961,-1.3083577072\C,-13.2567145692,-1.3488880942,-0.401886766\C
,-14.6310752883,-0.7006622679,-0.3204224659\H,-13.1542569471,-1.886451
3733,-1.358088767\H,-13.1441088173,-2.086190625,0.4090034898\H,-14.731
8011926,-0.1602025996,0.6344792766\H,-14.7448299852,0.0349314394,-1.13
28825623\C,-16.925622399,-1.2583982828,-0.3687585081\H,-17.1189570155,
-0.7342002582,0.5807669484\H,-17.1311018836,-0.5508226694,-1.187843048
7\O,-8.7083713052,-0.0619592735,-0.2795328024\O,-12.2919662597,-0.3197
320099,-0.2911590238\O,-15.5931477934,-1.7311252102,-0.426899984\C,-17
.8469785616,-2.4634983045,-0.4874447568\H,-17.641259605,-3.1709607347,
0.3328138053\H,-17.6505106862,-2.9898819571,-1.4361210234\C,-20.130484
599,-3.0247475559,-0.5309998263\H,-20.041771207,-3.5711195112,-1.48397
81435\H,-20.0324223488,-3.7499054937,0.2930781197\O,-19.1767359361,-1.
9894145801,-0.4319809969\H,-21.1183937822,-2.5595983713,-0.4789591014\

\Version=ES64L-G09RevD.01\State=1-A\HF=-2047.1093184\RMSD=4.311e-09\RMSF=1.152e-06\Dipole=0.192928,-1.1599695,-0.8442169\Quadrupole=38.1918353,-19.6310083,-18.560827,11.5400734,-6.4049453,-2.5218636\PG=C01 [X(C34H42F2O7)]\\@

s2

1\1\GINC-GAUSIANDELL\FOpt\RB3LYP\6-31G(d)\C27H44B11O2(1-)\PKASZYNSKI\23-Mar-2024\0\\#P B3LYP/6-31G(d) Fopt geom=(nodistance,noangle) SCF=direct\\CB11-1-CH2CH2C6H4OCOPh-Chx-C5\\-1,1\B,9.2308958428,-2.0907646025,-0.066922149\B,9.2655574546,-0.9751473221,1.3139234992\B,9.3236932261,-1.1249458385,-1.5521070392\B,9.3978909567,0.680614054,0.6849110808\B,9.4177598354,0.5864188215,-1.0880341722\B,10.9279001313,0.8320304974,-0.1893768072\B,10.8329479889,-0.1422751183,1.3100072936\B,10.8842999451,-0.2888897575,-1.5790888599\B,10.7644624454,-1.9549880598,-0.9414376923\B,10.7316594904,-1.8630209049,0.8438051576\B,11.7617838517,-0.7433200057,-0.0911548123\C,8.504338177,-0.5307169682,-0.1585688885\H,8.5048210573,-3.0365399172,-0.0297913633\H,8.5714773151,-1.1916135069,2.2610716408\H,8.6596246117,-1.4350923847,-2.4933705232\H,8.8124101768,1.5656083728,1.2233073768\H,8.8231407689,1.4006266384,-1.7279022496\H,11.5025075841,1.8790903629,-0.2325193157\H,11.3402582492,0.2121704798,2.3324066306\H,11.4271489832,-0.0400115845,-2.6143817716\H,11.2207764729,-2.8940187787,-1.5232179931\H,11.1660702618,-2.7358504018,1.5350864351\H,12.9547726217,-0.8189195569,-0.0648076425\C,6.969020727,-0.4936132707,-0.2324021862\H,6.671884149,-0.4418369648,-1.2861423933\H,6.5797795267,-1.4440669212,0.1502386518\C,6.2850885608,0.6607362835,0.5294298026\H,6.6550815248,1.6164592481,0.1436735875\H,6.5735252263,0.6161844272,1.5851401957\C,4.7781051321,0.6089975519,0.4075034774\C,4.0030581708,-0.1390233426,1.3057742448\C,4.1107306409,1.2848115409,-0.6235558964\C,2.6146953474,-0.2160595443,1.1947686346\C,2.7236355562,1.2245057305,-0.7511161894\C,1.986271799,0.4776113211,0.1630576851\O,0.6039913296,0.4020054058,-0.0725268674\H,4.4975475015,-0.6724097808,2.1142496148\H,4.6866796809,1.8706749701,-1.3360079054\H,2.0323991076,-0.7910884635,1.9043015165\H,2.2068514205,1.7500067228,-1.5487285052\C,-0.2936407447,0.5952615878,0.9328992083\O,0.0012958631,0.8171028991,2.0876373304\C,-1.6953146493,0.5035302644,0.4316986512\C,-2.7333817586,0.6879913165,1.3553956383\C,-2.0125321369,0.2516822907,-0.9086821333\C,-4.0602056517,0.6246371558,0.9455040576\H,-2.4758388494,0.8825809507,2.391452586\C,-3.3457438344,0.1902453186,-1.3094306665\H,-1.2159361678,0.1070295715,-1.6297052081\C,-4.3931485704,0.3758319553,-0.3965334138\H,-4.8479280533,0.7725928752,1.6799411387\H,-3.5792880472,-0.0045022284,-2.3538993728\C,-5.8395269711,0.3093722866,-0.8553637819\C,-6.6158987699,-0.8526818665,-0.1961849825\C,-6.5920269152,1.639816132,-0.6313576187\H,-5.8312709388,0.1198489836,-1.9393595662\C,-8.070820921,-0.9146719751,-0.6827013569\H,-6.6018736311,-0.7238115735,0.8954309464\H,-6.1051331317,-1.8016346363,-0.4018244004\C,-8.048468668,1.567437179,-1.1144409643\H,-6.5772480988,1.8884441039,0.4392839919\H,-6.0633383555,2.4532060759,-1.1438293105\C,-8.8274882047,0.4090301309,-0.4622908741\H,-8.5974773622,-1.7334868574,-0.1740928021\H,-8.0846558762,-1.1586848694,-1.7564083958\H,-8.5431962855,2.5256167975,-0.9138139237\H,-8.0638643172,1.4329451566,-2.2075416442\H,-8.8567998923,0.5965718908,0.6244783237\C,-10.2810086803,0.3040727059,-0.9599798915\C,-11.1854285295,1.490854365,-0.5978936264\H,-10.7248008588,-0.6134346766,-0.5455206079\H,-10.277188579,0.1696028304,-2.0527497314\C,-12.6423776453,1.297624378,-1.0387834548\H,-11.1549611727,1.6501028649,0.4905727151\H,-10.7962974498,2.4128426421,-1.0509954046\H,-12.6748062626,1.132452757,-2.1262809563\H,-13.0429033807,0.3800772066,-0.5819274099\C,-13.5536350471,2.4787896897,-0.6809557843\C,-15.006663601,2.2785920743,-1.1236539194\H,-13.1547467024,3.39527

7691,-1.138760355\H,-13.5215754501,2.6442055187,0.4054481969\H,-15.630
5711886,3.1384616072,-0.8535353862\H,-15.0752280434,2.1457743268,-2.21
05604369\H,-15.4450224083,1.3887587805,-0.6548473965\\Version=ES64L-G0
9RevD.01\State=1-A\HF=-1479.5389113\RMSD=5.210e-09\RMSF=3.775e-05\Dipo
le=-19.4655543,1.6482771,-0.7583526\Quadrupole=-247.9625631,121.786218
7,126.1763444,36.396546,-0.897124,-2.9432273\PG=C01 [X(C27H44B11O2)]\\
@

9. References

1 H. Fu, H. Li, Y. Li, Z. Lou, H. Yang, Y. Zhao, *Angew. Chem. Int. Ed.,* 2020, **59**, 3671–3677.

2 C. Wang, H. Wang, C. Zheng, B. Li, Z. Liu, L. Zhang, L. Yuan, P. Xu, *ACS Med. Chem. Lett.,* 2023, **14**, 92–102.

3 A. D. Becke, *J. Chem. Phys.,* 1993, **98**, 5648–5652.

4 C. Lee, W. Yang, R. G. Parr, *Phys. Rev. B,,* 1988, **37**, 785–789.

5 F. Weigend, *Phys. Chem. Chem. Phys.,* 2006, **8**, 1057–1065.

6 F. Weigend, R. Ahlrichs, *Phys. Chem. Chem. Phys.,* 2005, **7**, 3297–3305.

7 M. J. Frisch, G. W. Trucks, H. B. Schlegel, G. E. Scuseria, M. A. Robb, J. R. Cheeseman, G. Scalmani, V. Barone, B. Mennucci, G. A. Petersson, H. Nakatsuji, M. Caricato, X. Li, H. P. Hratchian, A. F. Izmaylov, J. Bloino, G. Zheng, J. L. Sonnenberg, M. Hada, M. Ehara, K. Toyota, R. Fukuda, J. Hasegawa, M. Ishida, T. Nakajima, Y. Honda, O. Kitao, H. Nakai, T. Vreven, J. A. Montgomery, Jr., J. E. Peralta, F. Ogliaro, M. Bearpark, J. J. Heyd, E. Brothers, K. N. Kudin, V. N. Staroverov, R. Kobayashi, J. Normand, K. Raghavachari, A. Rendell, J. C. Burant, S. S. Iyengar, J. Tomasi, M. Cossi, N. Rega, J. M. Millam, M. Klene, J. E. Knox, J. B. Cross, V. Bakken, C. Adamo, J. Jaramillo, R. Gomperts, R. E. Stratmann, O. Yazyev, A. J. Austin, R. Cammi, C. Pomelli, J. W. Ochterski, R. L. Martin, K. Morokuma, V. G. Zakrzewski, G. A. Voth, P. Salvador, J. J. Dannenberg, S. Dapprich, A. D. Daniels, O. Farkas, J. B. Foresman, J. V. Ortiz, J. Cioslowski, and D. J. Fox, Gaussian 09, Revision A.02, Gaussian, Inc., Wallingford CT, 2009.